PHASE PORTRAITS OF REAL QUADRATIC DIFFERENTIAL SYSTEMS POSSESSING AN INVARIANT ELLIPSE

JOAN C. ARTÉS[1], CRISTINA BUJAC[2], DANA SCHLOMIUK[3] AND NICOLAE VULPE[2]

Abstract. In this paper we construct the phase portraits of the family QSE of planar quadratic differential systems with real coefficients possessing an invariant ellipse (real or complex). To obtain them we needed to use several normal forms, modulo the action of the group of affine transformation and time rescaling. We produce the phase portraits of QSE in all the parameter spaces of its normal forms including the limit points of this family. We also produce the bifurcation diagram of QSE which contains phase portraits that are in the border of the normal forms. Although these border points do not contain an invariant ellipse they are needed to fully understand the phenomena involved. There are 40 phase portraits of quadratic systems which have an invariant ellipse and 5 which are on the border of the normal forms. A second result is a theorem which gives invariant conditions to determine if a quadratic system with an invariant ellipse, has one of the 40 phase portraits mentioned above, up to one case which cannot be completely decided by means of algebraic equations.

1. Introduction and statement of main results

We consider here differential systems of the form

$$\frac{dx}{dt} = p(x,y), \qquad \frac{dy}{dt} = q(x,y), \tag{1}$$

where $p,\ q \in \mathbb{R}[x,y]$, i.e. $p,\ q$ are polynomials in $x,\ y$ over $\mathbb{R}$. We call *degree* of a system (1) the integer $m = \max(\deg p, \deg q)$. In particular we call *quadratic* a differential system (1) with $m = 2$. We denote here by **QS** the whole class of real quadratic differential systems.

In his Memoir [4] Darboux introduced the notion of *particular algebraic solution* of a polynomial differential system and aplied it to construct their first integrals in case they exist. Later the term *algebraic particular integral* was also used. The theory of Darboux was far ahead of its time and it was only towards the end of the XX-th century and the beginning of this century that this area of research became very active. The term used in the curent literatire for *algebraic particular integral* is *algebraic invariant curve.*

Definition 1. *An algebraic invariant curve of a system* (1) *is a set* $\{(x,y) \in \mathbb{K}^2 | f(x,y) = 0\}$ *where* $\mathbb{K}$ *is* $\mathbb{R}$ *or* $\mathbb{C}$ *and* $f(x,y)$ *is a polynomial in* x, y *with coefficients in* $\mathbb{K}$ *(* $f(x,y) \in \mathbb{K}[x,y]$*) such that there exists* $L(x,y) \in \mathbb{K}[x,y]$ *called the cofactor of the curve* $f = 0$ *satisfying the following identity in* $\mathbb{K}[x,y]$*:*

$$f_x p(x,y) + f_y q(x,y) = f(x,y)L(x,y).$$

where f_x, f_y *are the partial derivatives of* f*.*

Apart from being important in the construction of first integrals of systems (1) algebraic invariant curves turn out to also be useful in constructing phase portraits of polynomial differential systems as we could have connections that lie on such curves. They are also interesting in their own right

2020 *Mathematics Subject Classification.* Primary 58K45, 34C05, 34A34.

Key words and phrases. quadratic vector fields, infinite and finite singularities, affine invariant polynomials, Poincaré compactification, configuration of singularities, topological equivalence relation.

and we have problems on systems possessing invariant algebraic curves that have been open for more than a century such as the problem of Poincaré [8].

A family of systems (1) important for applications is the Lotka-Volterra class which is defined by the property that its systems possess two affine invariant lines intersecting at a finite point. The phase portraits of this family were constructed in [10] based on the classification of its systems according to their configurations of invariant lines concept that includes their multiplicities.

In this article we consider the family QSE of systems (1) with coefficients in $\mathbb{R}$ possessing at least one invariant ellipse (real or complex). This family was previously studied in two papers [7] and [6].

Definition 2. *We call complex invariant ellipse of a polynomial differential system with real coefficients an invariant curve of degree two such that modulo a real affine transformation and time rescaling this invariant conic takes the form $x^2 + y^2 + 1 = 0$ in the new coordinates.*

In [7] the authors gave necessary and sufficient conditions for a quadratic differential system to have at least one invariant ellipse. They also provide a bifurcation diagram done in the space $\mathbb{R}^{12}$ of coefficients of the systems in QSE and expressed in terms of polynomial invariants. This bifurcation diagram tells us where there exists an invariant ellipse and where invariant ellipses are absent.

In [6] the authors gave a classification of the fami;y QSE in terms of their geometric properties encoded in their configurations of invariant ellipses and invariant lines. This classification is done modulo the action of the group of affine transformations and time rescaling and it is expressed in terms of polynomial invariants.

In this article we continue the work in these two papers. The goal of this article is to construct all the phase portraits of QSE. This family is not closed in the parameter space $\mathbb{R}^{12}$ and to fully understand its dynamics we also to study what happens at the limiting points of the space QSE and for this reason we consider the closure $\overline{QSE}$ in $\mathbb{R}^{12}$ and we construct all the phase portraits in the space $\overline{QSE}$ in $\mathbb{R}^{12}$.

Theorem 1. *We have a total of 45 topologically distinct phase portraits in the space $\overline{QSE}$ 40 of which are phase portraits of QSE.*

In [7] modulo this group action the family QSE was brought to two normal forms which we consider in our next section. The first one of these normal forms depends on four parameters and the second one on three parameters. After a rescaling to eliminate a denominator in the first normal form we study it using three-dimensional slices by giving specific constant values C to one of the four parameters, conveniently chosen. It turns out that if we adequatly choose the slicing parameter, due the group action, only two such 3-dimensional slices are necessary. This yields two 3-parameter sub-families covering the systems in the 4-dimensional first normal form. In Section 2 we denote these two families by $(\mathcal{A})$ and $(\mathcal{B})$. The second normal form in [7] depends on three parameters and we denote this third normal form with $(\mathcal{C})$.
All three 3-dimensional normal forms are studied here by using two-dimensional slices conveniently chosen by using the group action. We place the bifurcation diagrams of these three families on the resulting planar slices. To fully understand the dynamics we consider the closures $\overline{(\mathcal{A})}$, $\overline{(\mathcal{B})}$, $\overline{(\mathcal{C})}$ in their parameter spaces and their respective restrictions to the two-dimensional chosen slices.

Theorem 2. *The complete bifurcation diagrams of the four normal forms for the family QSE and its closure $\overline{QSE}$ in their respective parameter spaces is contained in eight diagrams of Section 4. The bifurcation sets split the parameter spaces into 171 distinct parts.*

In Figure 1 we have drawn the separatrices with thick lines, additional orbits with thin lines and graphics in blue. In case the ellipse is real, we have always drawn it according to the following

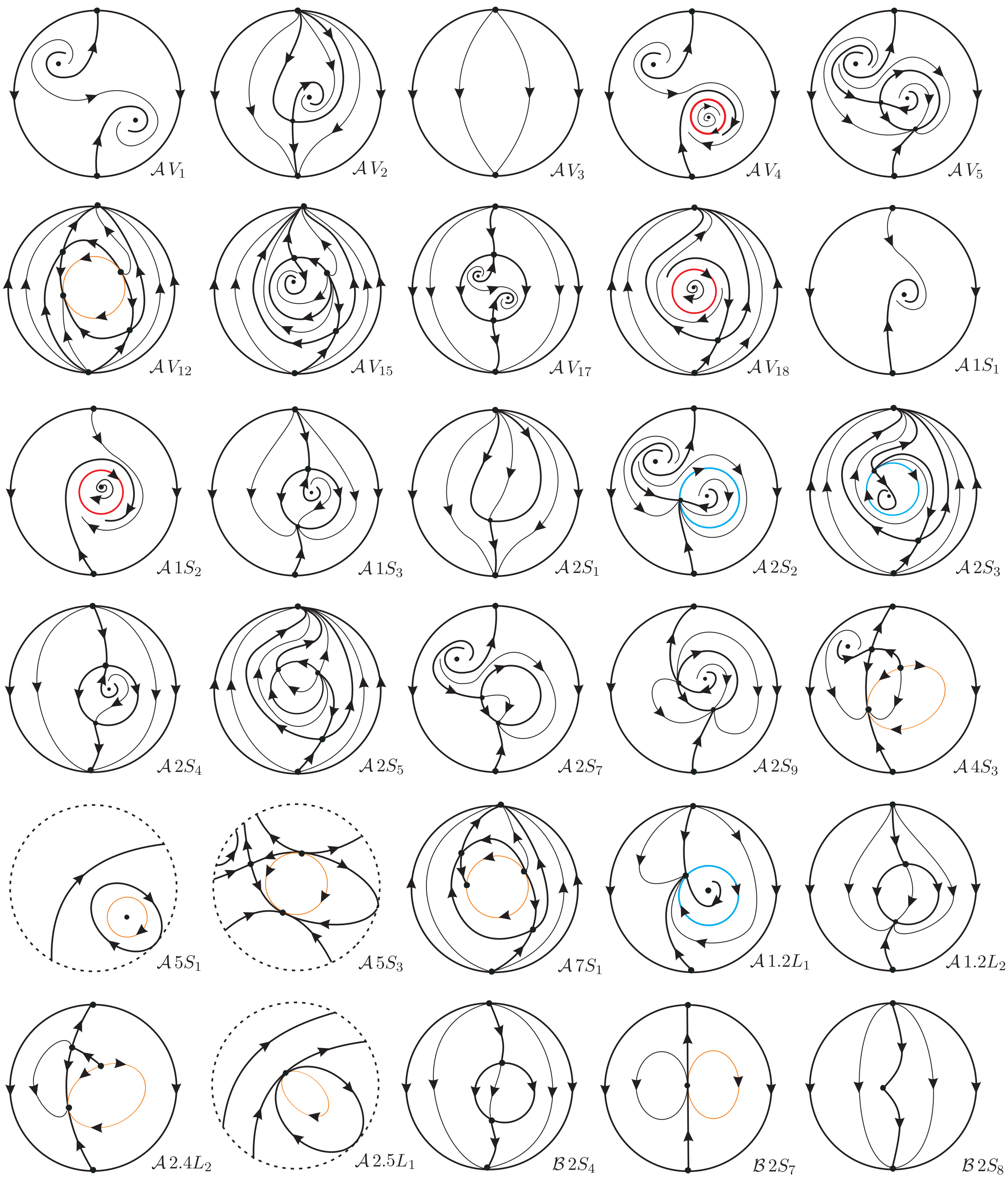

Figure 1. Phase portraits for the family $\overline{\mathbf{QSE}}$.

preference of colors: If the ellipse forms a graphic, in blue; if the ellipse is formed by separatrices but it is not a graphic, in black; if the ellipse is a limit cycle, in red, otherwise in orange.

From this result, one can extract the following theorem that determines the conditions for which any quadratic differential system having an invariant ellipse, will have one of the 40 phase portraits mentioned above, up to one case which cannot be completely decided by means of algebraic equations.

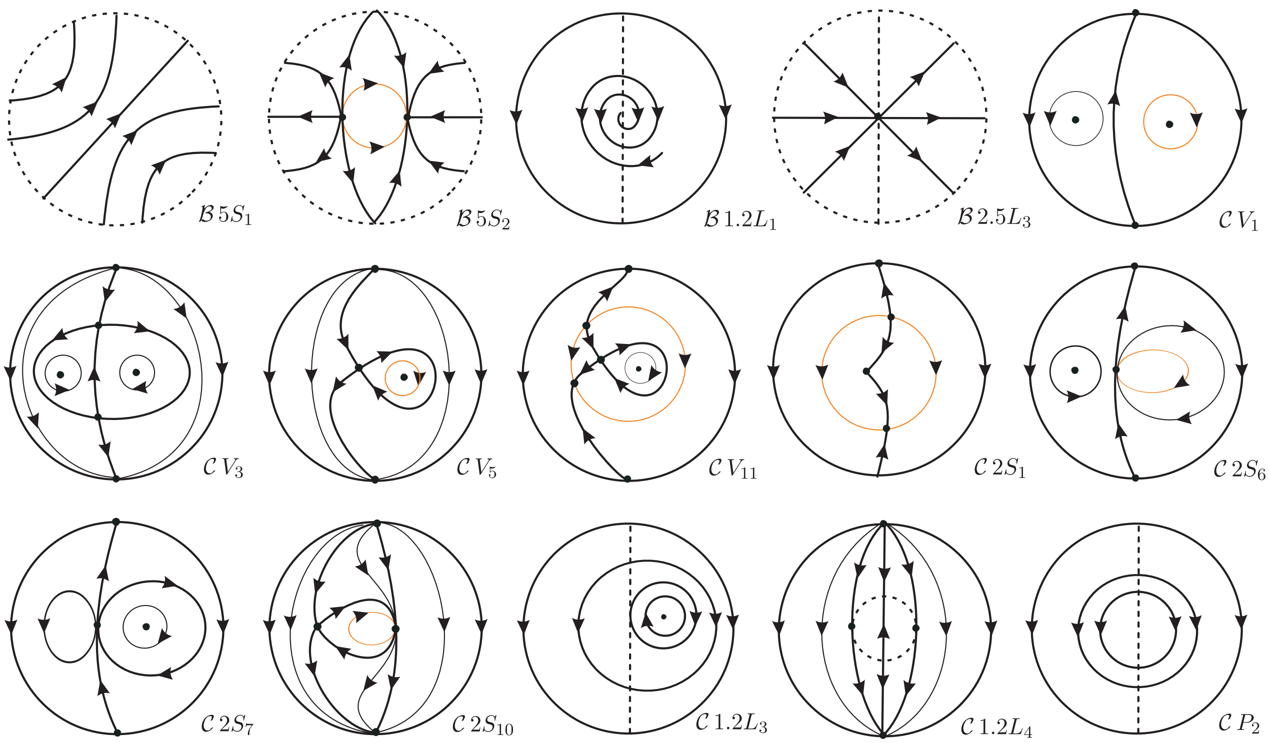

FIGURE 1 (*contin.*). Phase portraits for the family $\overline{\mathbf{QSE}}$.

Theorem 3. *Consider a quadratic system* (S) *in* $\mathbb{R}^{12}$. *If the set of conditions for any of the branches from* DIAGRAM *10 (see Section 6) for the existence of an invariant ellipse hold for system* (S), *then it will have one of the 40 distinct phase portraits from* DIAGRAM *11 (see Section 6) whose labels contain one of the two symbols* $\odot$ *or* $\bullet$. *The symbol* $\odot$ *indicates the presence of a real ellipse and* $\bullet$ *of a complex one.*

The paper is organized as follows. In Section 2 we construct the normal forms modulo the group action which are necessary for the work. In Section 3 we describe the different bifurcation surfaces which will split the parameter space for each one of the normal forms. The proof of Theorem 2 is done in Section 4 and Section 5. In the first of them, the bifurcation diagram for each one of the normal forms is constructed and the phase portraits in each specific part of it are determined. With the help of topological invariants, in Section 5 the number of topologically distinct phase portraits that have appeared among the 171 parts of the bifurcation diagram is determined.

In Section 6 we prove Theorem 3.

2. Normal forms

Consider the space QS of quadratic differential systems (1). To construct the normal forms for the family QSE we split this family according to the number of the distinct singularities the systems in this family have. The directions of the points at infinity of a system in QS are given by the equation $C_2(x, y) = yp_2(x, y) - xq_2(x, y) = 0$ where p_2, q_2 are the homogeneous polynomials of the degree two of p, q. We consider first the case $C_2 \neq 0$ in $\mathbb{R}[x, y]$. In this case the discriminant of C_2 is denoted with η. When the system varies in $\mathbb{R}^{12}$, η is a polynomial invariant with respect to the group action.

2.1. **The case $\eta < 0$ (only one infinite real singularity).** According to [7] a quadratic system possessing an invariant ellipse can be brought via an affine transformation and time rescaling to one of the following two canonical forms:

$$\dot{x} = a + dy + gx^2 + (h+1)xy, \quad \dot{y} = \frac{ah}{g} - dx - x^2 + gxy + hy^2, \quad ag \neq 0, \tag{$S^1_{\mathcal{E}}$}$$

possessing the invariant ellipse

$$\Phi(x,y) = \frac{a}{g} + x^2 + y^2 = 0, \tag{2}$$

or

$$\dot{x} = dy + (h+1)xy, \quad \dot{y} = b - dx - x^2 + hy^2, \quad bh \neq 0, \tag{$S^2_{\mathcal{E}}$}$$

possessing the invariant ellipse

$$\Phi(x,y) = \frac{b}{h} + x^2 + y^2 = 0. \tag{3}$$

We consider each one of these family of systems separately.

2.1.1. *The first canonical form* $(S^1_{\mathcal{E}})$. We want to apply a rescaling in order not to have a denominator in the coefficients of systems $(S^1_{\mathcal{E}})$. So we use the rescaling $(x,y) \mapsto (x/g, y/g)$ and setting $a = bm, g = 1/m, h = n/m$, where b, m and n are our new parameters (here $m \neq 0$ due to $g \neq 0$) we arrive at the following family of systems

$$\dot{x} = b + x^2 + dy + (m+n)xy, \quad \dot{y} = bn - dx - mx^2 + xy + ny^2, \quad \text{with} \quad bm \neq 0 \tag{4}$$

which possesses the invariant conic

$$\Phi(x,y) = b + x^2 + y^2 = 0. \tag{5}$$

We aim to reduce the number of parameters from four to three in order to handle the problem more efficiently. We can act with the group and apply for $d \neq 0$ the rescaling $(x,y,t) \to (dx, dy, t/d)$, we may assume without loss of generality that either $d = 1$ or $d = 0$. In the first case, we obtain the systems:

$$\dot{x} = b + x^2 + y + (m+n)xy, \quad \dot{y} = bn - x - mx^2 + xy + ny^2, \quad bm \neq 0 \tag{$\mathcal{A}$}$$

and in the second case we arrive at the systems:

$$\dot{x} = b + x^2 + (m+n)xy, \quad \dot{y} = bn - mx^2 + xy + ny^2, with \quad bm \neq 0 \tag{$\mathcal{B}$}$$

2.1.2. *The second canonical form* $(S^2_{\mathcal{E}})$. In this case the normal form already contains just 3 parameters and we will denote it by $(\mathcal{C})$.

2.2. **The case** $C_2 = 0$**.** According to [7], a quadratic system with $C_2 = 0$ may possess infinitely many invariant ellipses or none at all. As shown in [6], in the case where an infinite number of invariant ellipses exist, via an affine transformation and a time rescaling, the family can be brought to the following canonical form:

$$\dot{x} = a + dy + x^2, \quad \dot{y} = xy \tag{$\mathcal{D}$}$$

which admits the one-parameter family of invariant conics

$$\Phi_r(x,y) = a + 2dy + x^2 + ry^2 = 0. \tag{6}$$

We will show that all the phase portraits in this family have already appeared in the previously studied cases.

Proposition 1. *Let (S) be any quadratic system which coefficients in $\mathbb{R}^{12}$. Consider the tree of the bifurcation diagram* Diagram *10. Assume that the set of conditions for a branch of the tree in* Diagram *10 (see Section 6) for the existence of an invariant ellipse hold for the system (S). Then the system can be written in one of the normal forms $(\mathcal{A})$, $(\mathcal{B})$ or $(\mathcal{C})$.*

3. Bifurcation surfaces

At this stage, the classical approach begins by identifying the singularities, both finite and infinite of the normal form under study, along with their Jacobian matrices, determinants, traces, and discriminants. If the singularities are non-elementary, the appropriate classification theorems are applied, or blow-up techniques are employed. In the case of linear centers, Lyapunov constants are computed to determine whether the singularity is a true center surrounded by periodic orbits or a weak focus of a certain order.

The introduction of algebraic invariants applied to polynomial differential systems–particularly quadratic systems–has revolutionized the studies of Qualitative Theory. Previously, normal forms needed to be simple enough so that singularities could be computed using no more than square roots; otherwise, subsequent calculations became too complex to manage. The algebraic invariants, first employed in [1] and further developed in the comprehensive work [2], enable the straightforward detection of all varieties that signal bifurcations of the differential equation associated with singularities. For every geometric characteristic a singularity may exhibit, there exists one or more invariants governing it. Crucially, these invariants can be computed directly from any normal form without explicitly solving for the singularities. In addition, invariants that detect the existence of invariant straight lines have also been identified. While purely non-algebraic (or even non-analytic) features, such as certain separatrix connections or double limit cycles, cannot be detected by these algebraic invariants, their presence can be effectively inferred through coherence and continuity arguments once the algebraic bifurcation diagram is fully established.

***1:* Bifurcation surface corresponding to the coalescence of a finite singularity with a singularity at infinity.**

($\mathcal{S}_1$) The set of invariants that capture the conditions for which finite singularities escape to infinite is $\{\mu_0, \mu_1, \mu_2, \mu_3\}$ where the first non-zero μ_i is the relevant one.

For our families we have that

$$\begin{aligned} \mu_0^{(\mathcal{A})} &= -\, mn(1+(m+n)^2), \\ \mu_0^{(\mathcal{B})} &= -\, mn(1+(m+n)^2), \\ \mu_0^{(\mathcal{C})} &= -\, h(1+h)^2. \end{aligned} \tag{7}$$

So, we will define the surfaces:

$$\mathcal{S}_1^{(\mathcal{A})} = \mathcal{S}_1^{(\mathcal{B})}: \quad mn(1+(m+n)^2) = 0; \quad \mathcal{S}_1^{(\mathcal{C})}: \quad h(1+h) = 0,$$

and we will draw them in blue in all the bifurcation diagrams.

***2:* Bifurcation surface where at least two finite singularities coalesce.**

($\mathcal{S}_2$) The invariant that characterizes the coalescence of two finite singularities is denoted by $\mathbf{D}$. For our families we have that

$$\begin{aligned} \mathbf{D}^{(\mathcal{A})} =& 192(1+4bmn)(b+1+bm^2+2bmn+bn^2)\times \\ & (b+1+2bmn+2bn^2+n^2+bm^2n^2+2bmn^3+bn^4)^2, \\ \mathbf{D}^{(\mathcal{B})} =& 768b^4mn(1+mn+n^2)^4(1+m^2+2mn+n^2), \\ \mathbf{D}^{(\mathcal{C})} =& 192(4b+d^2)h(b+2bh+d^2h+bh^2)^3. \end{aligned} \tag{8}$$

So, we will define the surfaces:

$$\begin{aligned}\mathcal{S}_2^{(\mathcal{A})}:&\ (1+4bmn)(b+1+bm^2+2bmn+bn^2)\times\\&\ (b+1+2bmn+2bn^2+n^2+bm^2n^2+2bmn^3+bn^4)=0;\\\mathcal{S}_2^{(\mathcal{B})}:&\ bmn(1+mn+n^2)(1+m^2+2mn+n^2)=0;\\\mathcal{S}_2^{(\mathcal{C})}:&\ (4b+d^2)h(b+2bh+d^2h+bh^2)=0,\end{aligned}$$

and we will draw them in green in all the bifurcation diagrams.

***3:* Bifurcation surface on which the system has a weak finite singularity.**

($\mathcal{S}_3$) Classically, only weak foci were considered objects of interest in bifurcation diagrams, since they are non-elementary singularities whose perturbations may give rise to limit cycles. Weak saddles, on the other hand, appear rarely in such diagrams, as their topological effect is typically associated with the presence of a homoclinic loop passing through the same saddle. However, by Vulpe's Theorem [2, Theorem 6.2], it has been shown that weak saddles and weak foci are closely related objects, governed by the same set of invariants, even sharing the same notion of order of weakness. There also exist other invariants (such as $\mathcal{T}_3\mathcal{F}$) whose sign determines whether the detected weak singularity is a saddle or a focus.

In general, the invariant responsible for detecting weak singularities is $\mathcal{T}_4$; however, when this invariant vanishes, the subsequent ones ($\mathcal{T}_3, \mathcal{T}_2, \mathcal{T}_1$) become relevant, in the same manner as in the case of the μ_i invariants. For our families we have that

$$\begin{aligned}\mathcal{T}_3^{(\mathcal{A})}=&-m(9+m^2+6mn+9n^2)(b+1+bm^2+2bmn+bn^2),\\\mathcal{T}_4^{(\mathcal{B})}=&b^2m^2(3+m^2+4mn+3n^2)^2,\\\mathcal{T}_2^{(\mathcal{C})}=&-(1+3h)^2(b+2bh+d^2h+bh^2).\end{aligned}\tag{9}$$

We define the surfaces:

$$\begin{aligned}\mathcal{S}_3^{(\mathcal{A})}:&\ m(9+m^2+6mn+9n^2)(b+1+bm^2+2bmn+bn^2)=0;\\\mathcal{S}_3^{(\mathcal{B})}:&\ bm(3+m^2+4mn+3n^2)=0;\\\mathcal{S}_3^{(\mathcal{C})}:&\ (1+3h)(b+2bh+d^2h+bh^2)=0,\end{aligned}$$

and we will draw them in yellow in all the bifurcation diagrams. However, if the surface happens to be not relevant for topological changes, we will draw it with dashes.

***4:* Existence of an invariant straight line.**

($\mathcal{S}_4$) All points for which the corresponding phase portraits possess an invariant line form a surface strictly contained in the surface ($\mathcal{S}_4$) defined further below.

Furthermore, the invariant line may either coincide with a separatrix connection — making it topologically relevant — or not. The occurrence of this invariant line is determined by the set of comitants B_1, B_2 and B_3 defined in [9], some calculated below for the three canonical forms.

$$\begin{aligned}B_1^{(\mathcal{A})}=&-b^2m^3(1+n^2)(1+m^2-2mn+n^2)^2(1+bm^2+2bmn+bn^2),\\B_1^{(\mathcal{B})}=&-b^3m^3(m+n)^2(1+n^2)(1+m^2-2mn+n^2)^2,\\B_2^{(\mathcal{C})}=&-648b^2(-1+h)^4x^4.\end{aligned}\tag{10}$$

We define the surfaces:

$$\mathcal{S}_4^{(\mathcal{A})}: \ bm(1+n^2)(1+m^2-2mn+n^2)(1+bm^2+2bmn+bn^2)=0;$$
$$\mathcal{S}_4^{(\mathcal{B})}: \ bm(m+n)(1+n^2)(1+m^2-2mn+n^2)=0;$$
$$\mathcal{S}_4^{(\mathcal{C})}: \ b(-1+h)=0,$$

and they will be represented in solid magenta when they correspond to a separatrix connection, and in dashed magenta when they do not.

***5:* Bifurcation surface where at least two infinite singularities coalesce.**

($\mathcal{S}_5$) The invariant that captures the coalescence of two infinite singularities is η and in case it is zero, the comitants $\widetilde{M}$ and C_2 intervene. In our cases we have:

$$\begin{aligned}\eta^{(\mathcal{A})} &= -\,4m^4,\\ \eta^{(\mathcal{B})} &= -\,4m^4,\\ \eta^{(\mathcal{C})} &= -\,4.\end{aligned} \tag{11}$$

We define the surfaces:

$$\mathcal{S}_5^{(\mathcal{A})} = \mathcal{S}_5^{(\mathcal{B})}: \quad m=0,$$

and we will draw it in red. Notice that, in the case of the normal form ($\mathcal{C}$), the invariant $\eta^{(\mathcal{C})} = -4 \neq 0$, which implies the existence of a single real singularity at infinity.

***6:* Non algebraic bifurcation.** Finally, in one of the normal forms, there exists another bifurcation surface which is non-algebraic (and possibly also non-analytic) on which a separatrix connection occurs. We denote this surface by $\mathcal{S}_7$, and we will represent it in solid magenta, as for $\mathcal{S}_4$, since both correspond to separatrix connections. However, the labels of the regions — whether $4S_i$ or $7S_i$ — will indicate the specific type of connection involved. The presence of this surface can only be determined through coherence arguments, as will be shown in Section 4.

***7:* Notation for the regions of the bifurcation diagram.** Following the style used in several previous papers we have denoted the diferent parts of the bifurcation diagram in the following way:

- The 3-dimensional parts are denoted as V_i (V for "Volume");
- The 2-dimensional parts are denoted as xS_i (S for "Surface") where x is the number of the surface and i is a counter. Then a part named $1S_i$ means that a finite singularity has escaped to infinity; a part named $2S_i$ means that two finite singularities have coalesced. Moreover, these parts are colored as explained above;
- The 1-dimensional parts are denoted as $x.yL_i$ (L for "Line") where x and y are the numbers of the surfaces that pass through that part and i is a counter. It is possible that $x=y$ and then this means that such a part is a singular variety of one surface. In case that three of more surfaces pass through a same 1-dimensional part, we have chosen the codes of the two most relevant ones from a geometric point of view.
- The 0-dimensional parts (which can only be found in the singular slices) are denoted as P_i (P for "Point") where i is a counter.
- If a part is not yet fully determined because we will later determine the existence of a non algebraic bifurcation, the letter from the set (V, S, L, P) used is written in lower case. In case it is not going to change, it is already written in capital case.

This notation has proven to be very useful in past papers since we have always used the same codes and the same colors to indicate the different surfaces. So, it becomes very easy for a trained reader to see the bifurcation diagram and immediately forsee some of the topological features that one is going to find in that phase portrait. This helps to detect easily inconsistencies and avoid errors.

4. Bifurcation diagrams

In this section we will describe one by one all the bifurcation diagrams for each of the three different normal forms we have produced in Section 2 and with the help of the bifurcation surfaces we have already computed in Section 3. We do each one in independent subsections.

Since we are studying 3-dimensional normal forms, one must divide the parameter space in slices (by choosing a convenient parameter) as it has been done in other similar studies like [1] and others, and distinguishing between generic slices (where the topological behavior of the phase portraits do not change from one slice to close enough ones), and singular slices which contain some point of intersection of several bifurcation surfaces, and thus, there may appear different phase portraits on slices as close as wished to the singular slice. In some papers, the number of singular slices (and consequently, the number of generic slices) ran into several dozens, giving thus very rich bifurcation diagrams. However, for our three normal forms it is relatively easy to prove that they all have a unique singular slice ($n = 0$ for (A), $b = 0$ for (B) and $d = 0$ for (C)), so we need very few slices in each case.

We start with the most complicate bifurcation diagram, and the only one that contains a non algebraic bifurcation surface.

4.1. **Bifurcation diagram for normal form** $(\mathcal{A})$**.** We decide to make slices according to the parameter n and then we find that the only singular slice occurs for $n = 0$ (where $\mu_0 = 0$).

Generic slice: Thus we take a simple value for $n \neq 0$, let us say $n = 1$, and plot all the intersections of the bifurcation surfaces with this slice (which will be planar polynomial curves). Some of the regions that we obtain can be very small, their images we give in Diagram 1 are somewhat enlarged but topologically equivalent to them. In any case, we have preserved the situation when two surfaces are tangent.

In the diagram, we have not added the letter "$\mathcal{A}$" in every label, so as not to overcharge the image. However, the pictures in Figure 1, include the character which identifies from which normal form comes everyone of the phase phase portraits.

Next, we employ the numerical program P4 [5] to obtain the phase portrait corresponding to each region. During this process, it becomes apparent that some of the phase portraits $\mathcal{A}\,4S_i$ obtained for the subregions $4S_i$ are not topologically distinct from those of the neighboring regions bounded by these parts. The reason is that the invariant straight line represented by the surface $\mathcal{S}_4$ does not, in most cases, correspond to a separatrix connection. In fact, only in the subregion $4S_3$ does a separatrix connection occur, yielding a phase portrait $\mathcal{A}\,4S_3$ that differs from $\mathcal{A}\,V_{10}$ and $\mathcal{A}\,V_{11}$. Thus we draw the purple curve in solid line when it really produces a topological change, and in dashed mode when it does not. A similar phenomenon happens often with surface $\mathcal{S}_3$ when the property captured by it is not the presence of a weak focus but of a weak saddle. And, very interestingly, in a slice of normal form $\mathcal{B}$ we will see a situation in which the surface $\mathcal{S}_2$ is not relevant.

Then one must compare the phase portraits obtained for the different surfaces, and check if they are compatible with those obtained in the adjacent two dimensional regions.

After this detailed check one discovers that the only incoherence happens around regions v_{13}, v_{14} and $4s_5$ whose phase portraits are topologically equivalent to the one in V_{12}. We have denoted these regions in lowercase letters so as to remark their provisional status. The reason is that the phase portrait that one may obtain by perturbing $\mathcal{A}5S_3$ when entering v_{13} is not compatible with the one we have in $2S_6$, whose phase portrait is topologically equivalent to the one in $2S_5$. The disappearance

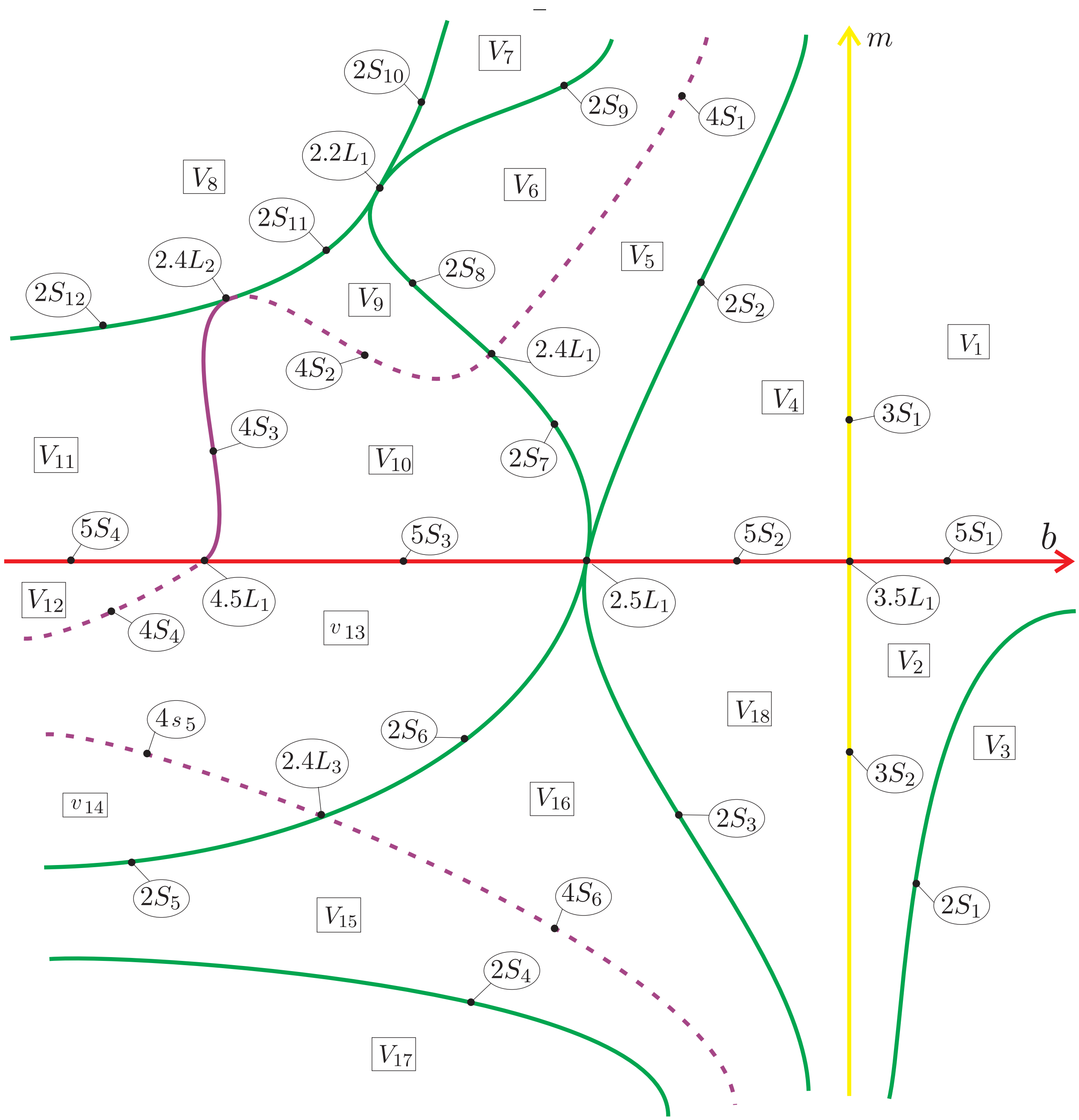

Diagram 1. Provisional bifurcation diagram for system ($\mathcal{A}$): slice $n = 1$.

of the saddle-node in $2S_5$ does not produce the phase portrait $\mathcal{A}\,V_{13}$ but a new phase portrait which we denote by $\mathcal{A}\,V_{19}$. And consequently, there must exist a bifurcation surface $\mathcal{S}_7$ which captures a possibly non algebraic separatrix connection between both finite saddles, giving then the phase portrait $\mathcal{A}\,7S_1$ (see Diagram 2) where the part $7S_1$ splits the previous region v_{13} in two subregions V_{13} and V_{19}. Next, one needs to check by numerical tools and arguments of coherence, where this surface starts and ends. It must be the border between V_{13} and V_{19}, it cannot cross surface $\mathcal{S}_2$ because the separatrices involved in the connection, become compromised by the existence of the saddle-node. It can neither cross $5S_3$ (nor $5S_4$ nor $4.5L_3$) because the saddle which has escaped to infinity in $\mathcal{A}\,5S_3$ sends the separatrix which should make the connection to a finite node. Hence a perturbation of $\mathcal{A}5S_3$ cannot produce $\mathcal{A}\,7S_1$. Thus the only remaining possibility is that $7S_1$ ends

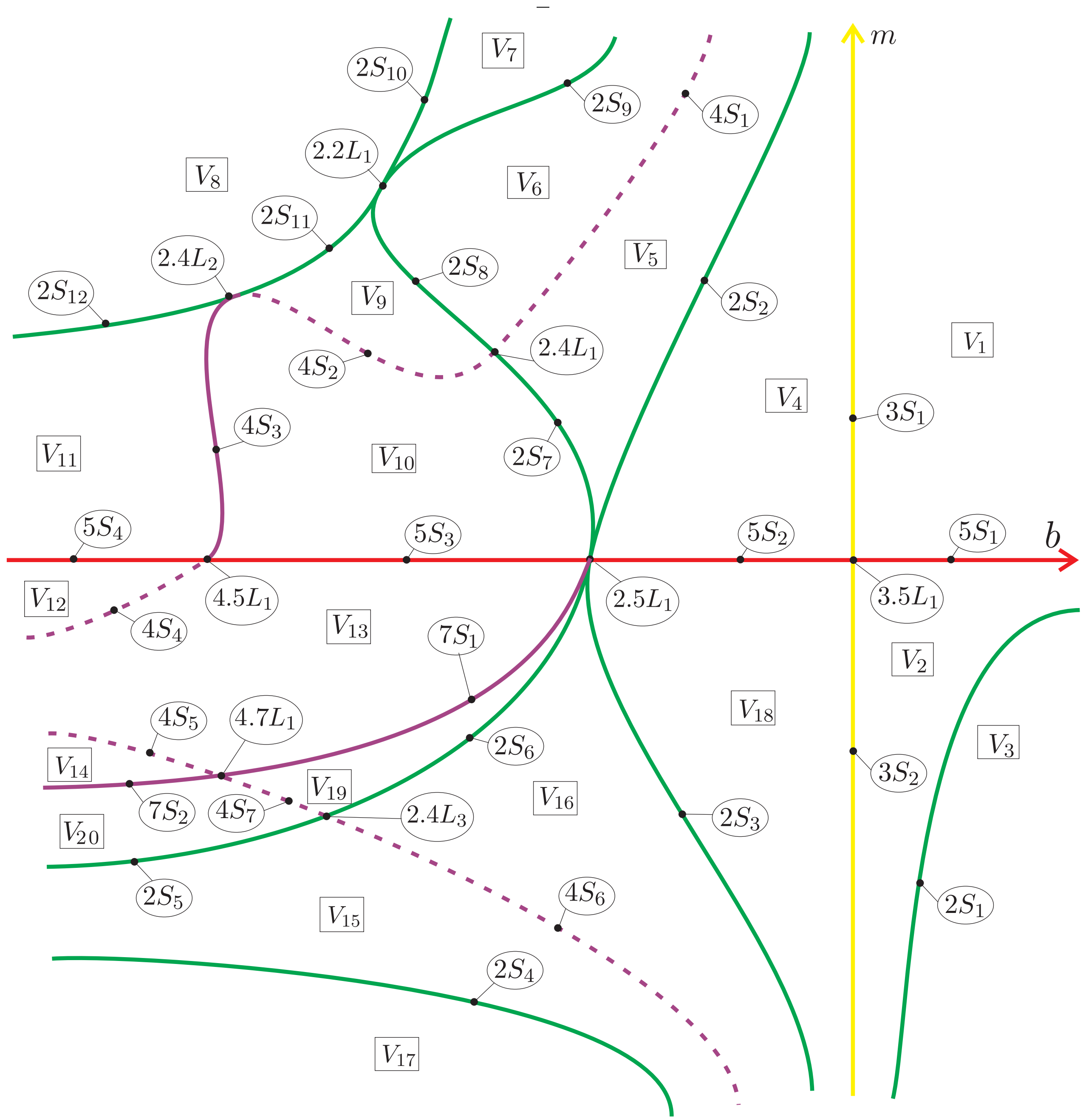

Diagram 2. Bifurcation diagram for system $(\mathcal{A})$: slice $n = 1$.

on $2.5L_1$ which produces a phase portrait compatible by perturbation with $\mathcal{A}\,7S_1$. And for the other side, part $7S_1$ is restricted between surfaces $\mathcal{S}_2$ and $\mathcal{S}_5$, then $\mathcal{S}_7$ must go to infinity with the same asymptotic behavior of the other two. But given that $7S_1$ is very close to $2S_6$ (numerical checking) it is perfectly possible that surface $\mathcal{S}_7$ crosses $4s_5$ (becoming then $7S_2$) and splits the region v_{14} in regions V_{14} and V_{20}, splitting also $4s_5$ into $4S_5$ and $4S_7$, plus a new 1-dimensional curve $4.7L_1$. Since on these regions, the surface $\mathcal{S}_4$ has no topological relevance, we have that the phase portraits for regions V_{19}, V_{20} and $4S_7$ are topologically equivalent to the phase portrait $\mathcal{A}V_{19}$, and the phase portrait for regions $7S_1$, $7S_2$ and $4.7L_1$ are topologically equivalent to the phase portrait $\mathcal{A}7S_1$.

There is an interesting phenomenon to remark in this diagram. In all the generic three-dimensional regions (except one), we obtain a codimension 0 (structurally stable) phase portrait. But in region

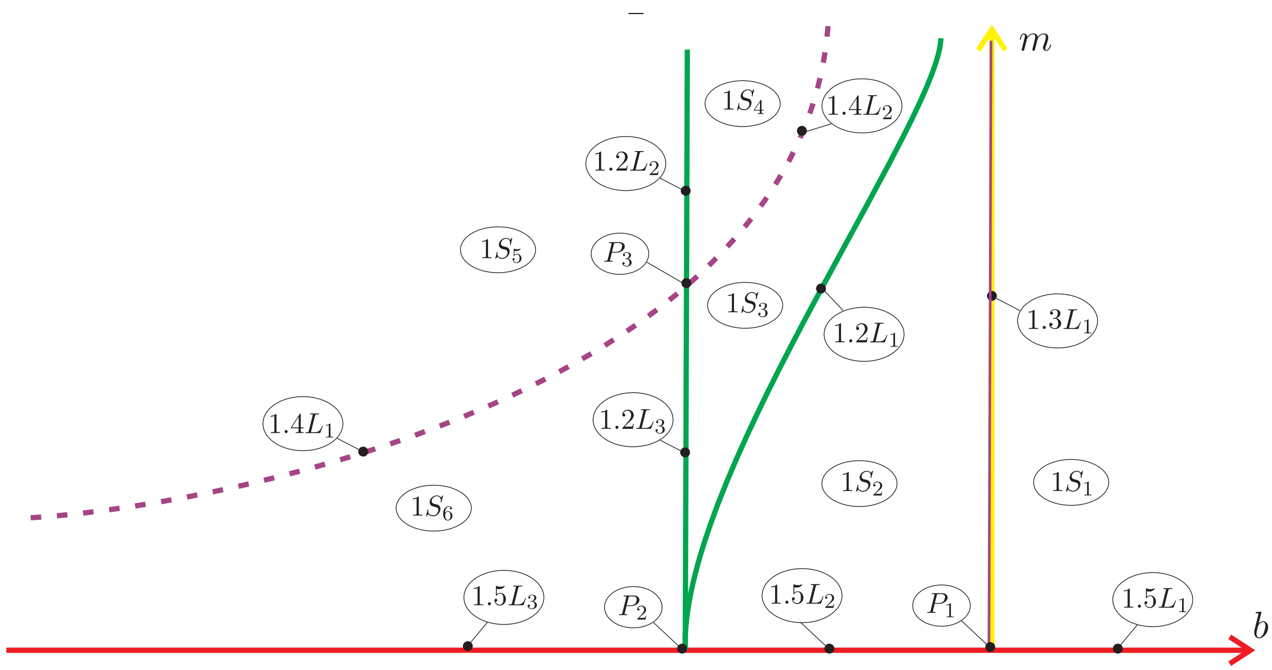

Diagram 3. Bifurcation diagram for system $(\mathcal{A})$: slice $n = 0$.

V_{17} we get a codimension 2 phase portrait with two separatrix connections. This is rarely occurring when studying this kind of bifurcations diagrams. The explanation comes from the fact that we are working with a normal form that always contains an invariant ellipse (real or complex) and this is not geometrically stable. There are always two singular points (real or complex) located on the ellipse. When these two singular points are complex, this produces no topological effect. When these two singular points are a real saddle and a real node, neither this produces a topological effect. But, in region V_{17} it happens that both saddles are on the ellipse, and thus the ellipse itself forces the existence of the two separatrix connections. By continuity, also the phase portrait in the region $2S_4$ has codimension 3 instead of 1 because the saddle-node is on the ellipse and maintains the same separatrix connections as in V_{17}. However, when we move into V_{15} the saddle-node splits into a saddle and a node and the node remains on the ellipse, but this saddle escapes outside. However, the other saddle still remains on the ellipse and two of its separatrices still form the ellipse. So, both separatrix connections get broken when entering in V_{15}.

Singular slice: Now we take $n = 0$ in normal form $(\mathcal{A})$ and we proceed in a similar way. It is simple to detect that there is a symmetry between the semi-plane $m > 0$ and $m < 0$, so we only draw the semi-plane $m \geq 0$ and obtain Diagram 3. Here the two-dimensional regions are really two-dimensional in the whole parameter space and correspond to pieces of the surface $\mathcal{S}_1$, so they are denoted as $1S_i$. The segments we see are intersections of other surfaces with $\mathcal{S}_1$ and are denoted as $1.jL_i$, with j corresponding to the most topologically relevant surface that intersects $\mathcal{S}_1$ in case there are more than one. Finally, the points P_1, P_2 and P_3 are intersections among three (or more) surfaces. Notice also that the vertical axis $b = 0$ has been drawn simultaneous in yellow and purple to denote that it is part of surfaces $\mathcal{S}_3$ and $\mathcal{S}_4$.

In this case, there is no lack of coherence and there is no need of the existence of a non algebraic bifurcation to explain all the diagram. In any case, there is always the possibility of the existence of islands in any of the bifurcation diagrams.

4.2. **Bifurcation diagram for normal form** $(\mathcal{B})$**.** We decide to make slices according to the parameter b and then we find that the only singular slice occurs for $b = 0$ (where $\mathbf{D} = 0$). We need then to study two generic slices $b > 0$, $b < 0$ and a singular one $b = 0$.

Generic slices: We can study both generic slices simultaneously since they are very similar with few differences. Due to a time rescaling $(x, y, t) \to (|b|^{1/2}x, |b|^{1/2}y, |b|^{-1/2}t)$ we may assume $b = 1$ for the generic slices $b > 0$ and $b = -1$ for the $b < 0$ ones. The bifurcation curves obtained by intersecting the bifurcation surfaces with these slices produce exactly the same equations. However, in Diagram 4 we have drawn the green bifurcation (different from the horizontal axis) as a dashed curve and in Diagram 5 we have drawn it solid. The difference is that for $b = 1$ this component of $\mathcal{S}_2$ corresponds to a case with two double complex finite singularities, and thus, this does not produce any topological effect. On the other hand, for $b = -1$ this same component produces two double real singularities, that is, two saddle-nodes, and this becomes a topological bifurcation in that slice.

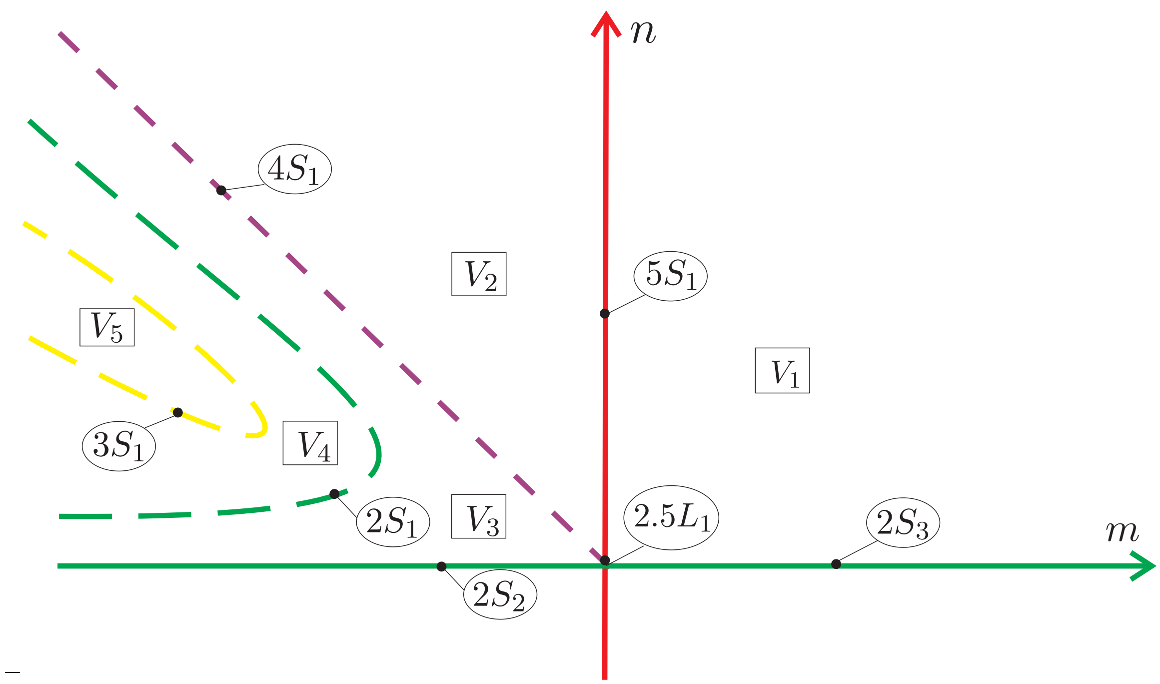

Diagram 4. Bifurcation diagram for system $(\mathcal{B})$: slice $b = 1$

In both slices, the component of $\mathcal{S}_3$ corresponds to a case with weak saddle, and in none slice, this is topologically relevant.

The nomenclature of regions follows the same pattern as described for the normal form $(\mathcal{A})$.

In this case, we detect that there is coherence among all the neighbor regions, and there is no need of non-algebraic bifurcations.

Singular slice: The slice $b = 0$ produces a very simple Diagram 6 where the most relevant feature is that all the slice is contained inside the bifurcation $\mathcal{S}_2$.

4.3. **Bifurcation diagram for normal form** $(\mathcal{C})$**.** We recall that the systems $(\mathcal{C})$ are defined as $(S^2_{\mathcal{E}})$, i.e. we consider the two-parameter family

$$\dot{x} = dy + (h+1)xy, \quad \dot{y} = b - dx - x^2 + hy^2, \qquad (\mathcal{C})$$

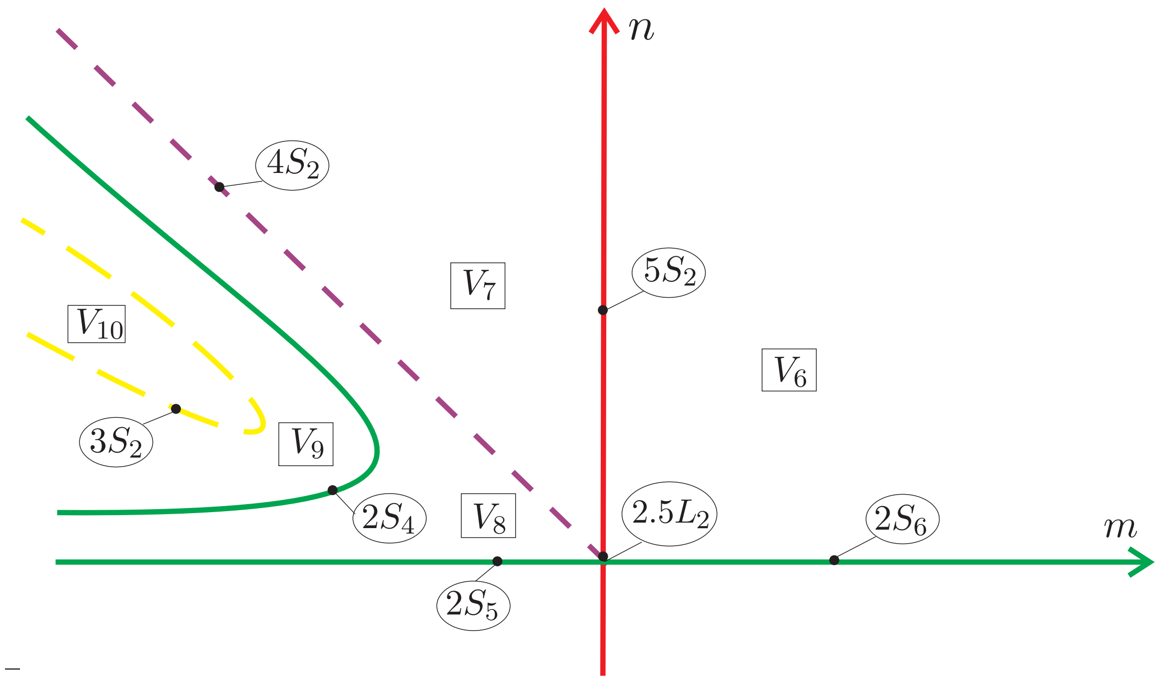

Diagram 5. Bifurcation diagram for system ($\mathcal{B}$): slice $b = -1$

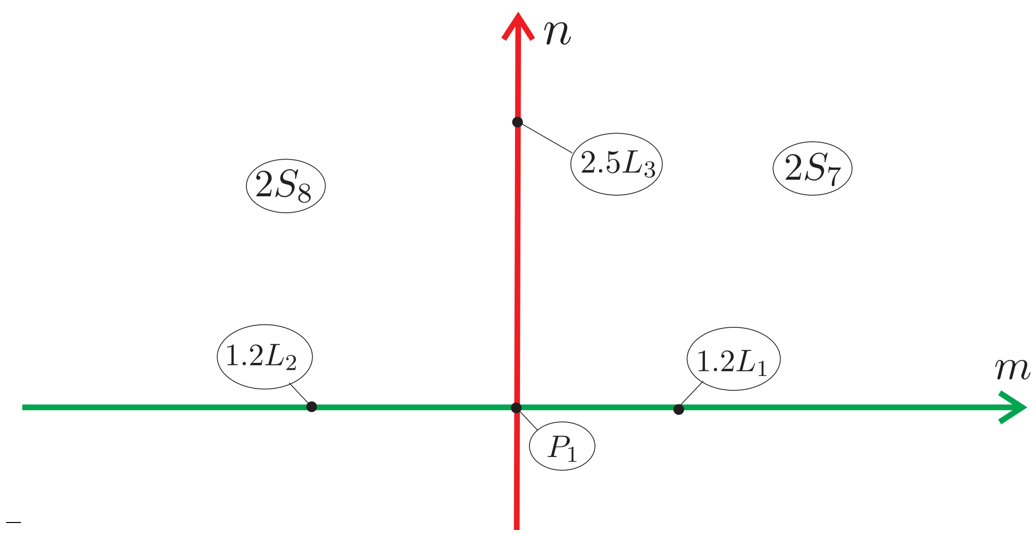

Diagram 6. Bifurcation diagram for system ($\mathcal{B}$): slice $b = 0$

Due to the change $x \to -x$ we can change the sign of parameter d. We chose to make slices $d = C$ where C is a constant and then we find that the only singular slice occurs for $d = 0$ (where several bifurcation surfaces coincide).

Generic slice: Thus we take a simple value for $d \neq 0$, let us say $d = 1$, and plot all the intersections of the bifurcation surfaces with this slice (which will be planar polynomial curves). We get the image given in Diagram 7 where the most relevant fact is the coincidence between components of some bifurcations, for example, surfaces $\mathcal{S}_1$ and $\mathcal{S}_2$ have a common component on the horizontal axis and surfaces $\mathcal{S}_2$ and $\mathcal{S}_3$ have a common cubic component. We have named the horizontal axis as belonging to the surface $\mathcal{S}_1$ and the mentioned cubic component as belonging to the surface $\mathcal{S}_2$ according to the more relevant bifurcation criteria.

In this case, we again detect that there is coherence among all the neighbor regions, and there is no need of non-algebraic bifurcations.

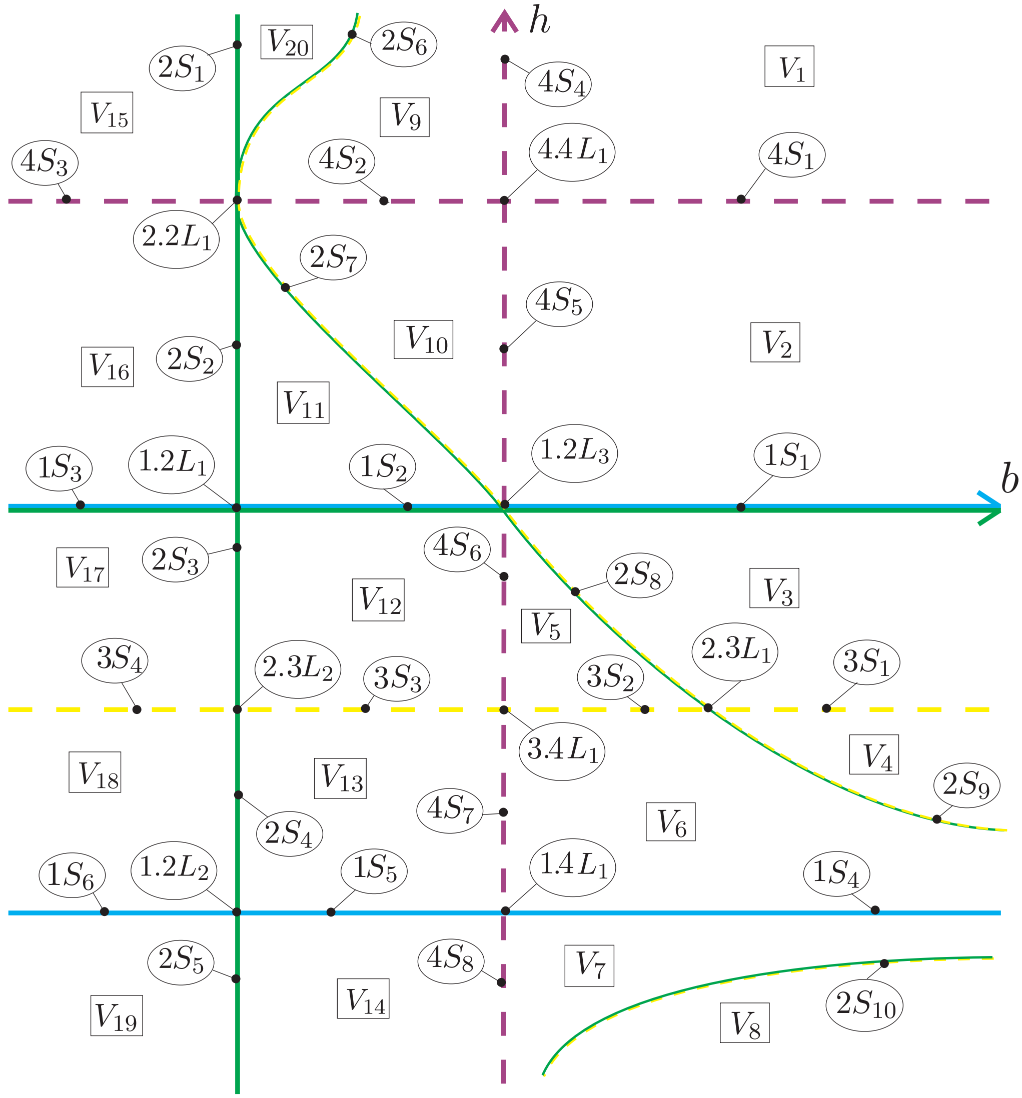

DIAGRAM 7. Bifurcation diagram for system $(\mathcal{C})$: slice $d = 1$

Singular slice: The slice $d = 0$ produces a very simple DIAGRAM 8 where the most relevant feature is that the vertical green line we had on DIAGRAM 7 has coalesced with the vertical axis (a component of $\mathcal{S}_4$). Also the cubic common component of $\mathcal{S}_2$ and $\mathcal{S}_3$ has coalesced with the vertical axis and the component $h = -1$ of $\mathcal{S}_1$.

This singular slice is not part of a bifurcation surface as it happened with the singular slices of the two previous normal forms. Then the parts with $b > 0$ and $b < 0$ with $h \neq -1$ are inherited from the generic slice. Only the names of the parts in $b = 0$ or $h = -1$ change according to the already mentioned criteria.

There is no need of a non-algebraic bifurcation and the study of the bifurcation diagram is complete.

4.4. **Bifurcation diagram for normal form** $(\mathcal{D})$**.** The normal form $(\mathcal{D})$ is very simple to study, and it can be completely done at the algebraic invariant level. In order to do it, one simply needs to compute the following algebraic invariant polynomials from [3] applying the diagrams from this book.

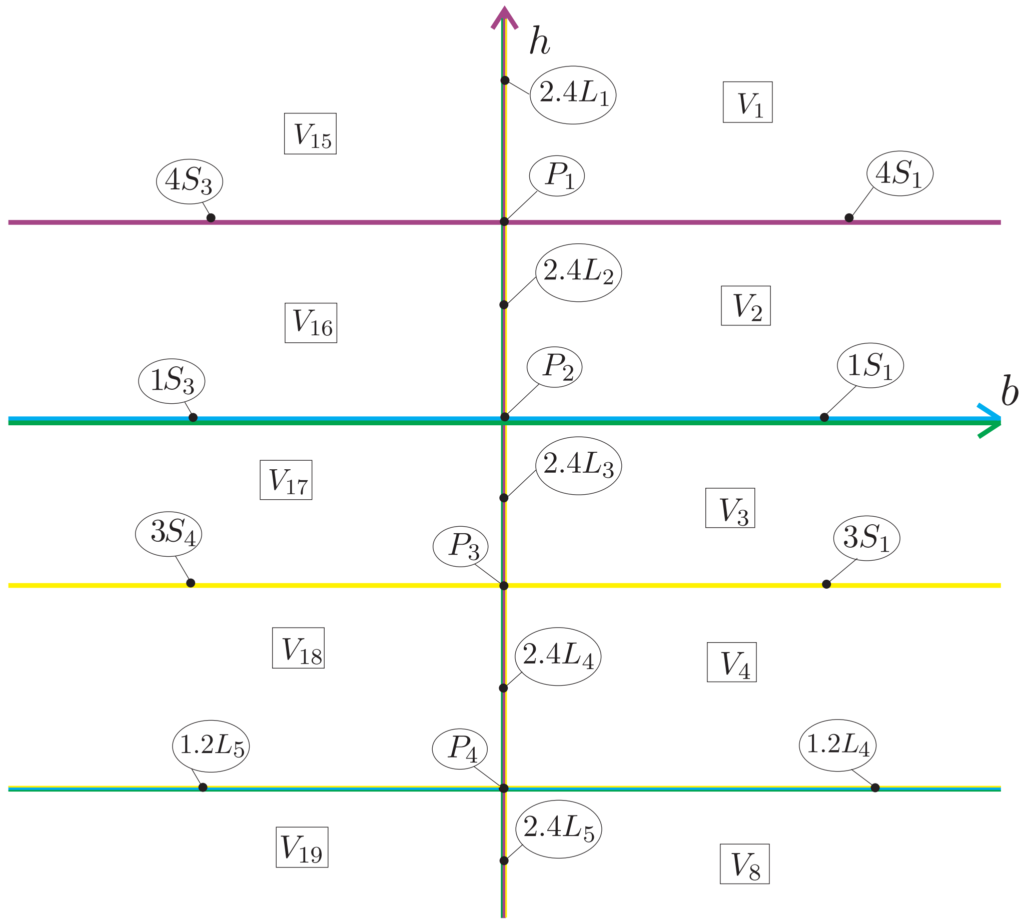

Diagram 8. Bifurcation diagram for system $(\mathcal{C})$:: slice $d = 0$

For the whole family the following invariant polynomials have fixed values:

$$\mu_0 = \kappa = \mathcal{B}_1 = \mathcal{F}_1 = \tilde{L} = \eta = \widetilde{M} = C_2 = 0, \ \widetilde{K} = 2x^2.$$

In case $d \neq 0$, we will need also the following invariant polynomials:

$$\mu_1 = dx, \ \mathbf{D} = 192a^3d^2, \ \mathbf{P} = ax^2(a^2x^2 - 3d^2y^2), \ W_7 = -3a^3d^4/4.$$

If $d = 0$ we will need the following additional invariant polynomials:

$$\mu_1 = \mu_3 = 0, \ \mu_2 = ax^2, \ \mu_4 = a^2x^2y^2, \ \mathbf{U} = -4a^3x^4y^2, \ K_2 = -192ax^2.$$

With these invariant polynomials and by using the diagrams in [3] it becomes very simple to determine the global geometric configurations of singularities according to some very simple inequalities. There are just 6 possible configurations, and each one of these configurations has a unique phase portrait which has already appeared in one of the previous normals forms. More concretely we have that $\operatorname{sign}(d) = \operatorname{sign}(\mu_1)$, if $\mu_1 \neq 0$ then $\operatorname{sign}(a) = \operatorname{sign}(\mathbf{D})$ and if $\mu_1 = 0$ then $\operatorname{sign}(a) = \operatorname{sign}(\mathbf{U})$. So we obtain the following phase portraits:

$$\begin{array}{llll}
\mu_1 \neq 0, \ \mathbf{D} < 0 & \Rightarrow \ \mathcal{A}\,5S_3, & \qquad \mu_1 = 0, \ \mathbf{U} < 0 & \Rightarrow \ \mathcal{B}\,5S_1, \\
\mu_1 \neq 0, \ \mathbf{D} > 0 & \Rightarrow \ \mathcal{A}\,5S_1, & \qquad \mu_1 = 0, \ \mathbf{U} > 0 & \Rightarrow \ \mathcal{B}\,5S_2, \\
\mu_1 \neq 0, \ \mathbf{D} = 0 & \Rightarrow \ \mathcal{A}\,2.5L_1, & \qquad \mu_1 = 0, \ \mathbf{U} = 0 & \Rightarrow \ \mathcal{B}\,2.5L_3.
\end{array}$$

5. Use of topological invariants

Up to here, we have divided the parameter space of 3 normal forms into 171 different parts, among which 50 three-dimensional parts, 75 two-dimensional parts, 38 one-dimensional parts and 8 zero-dimensional parts. We have already detected that some neighbor phase portraits are topologically equivalent, but it is not so simple to detect if two far away regions have the same phase portrait. Too many times, authors have tried to detect similarities between a set of phase portraits from a given classification, and doing it by simple visual check has lead to repetitions of phase portraits. In order to avoid this, we are going to introduce some topological invariants I_j with $1 \leq i \leq 4$ which will help us to decide if two given phase portraits are distinct.

Definition 3. Let $I_1(S)$ denote a number $n \in \mathbb{N}$ introduced in [3] associated with the topological configuration of singularities of a phase portrait mentioned in [3, Diagrams 1-6]. For example $I_1(S) = 12$ means that the phase portrait has no real finite singularity and just one infinite node, or $I_1(S) = 98$ means that there is a finite saddle-node plus a finite anti-saddle, and an infinite saddle-node obtained by the coalescence of a finite and an infinite singularities. Or an example of even more degenerated configuration: $I_1(S) = 175$ means that the phase portrait has an infinite number of finite singularities forming an invariant ellipse with no other finite singularity, plus an infinite node. In this way, two phase portraits having different codes by the topological invariant I_1 are clearly topologically distinct.

Definition 4. Let $I_2(S)$ denote a code given by the sequence of up to four digits (each one ranging from 0 to 5) such that each digit describes the total number of global or local separatrices ending at (or starting from) a singular finite point. The digits are ordered in descending order. In case there is no real finite singularity, we say that the invariant is equal to “null”.

In all previous papers we use a third invariant $I_3(S)$ similar to $I_2(S)$ related to the separatrices going to infinite singular points. In this paper we do not need it but we want to preserve the number given to each invariant so to facilitate the compatibility among papers.

Definition 5. Let $I_4(S)$ denote a digit that gives the number of limit cycles around a focus.

Remark 1. *The phase portraits having neither limit cycles nor graphicschave been denoted surrounded by parenthesis, for example* $(\mathcal{A}\,V_1)$*; the phase portraits having a limit cycle have been denoted surrounded by brackets, for example* $[\mathcal{A}\,V_4]$*; the phase portraits having graphics have been denoted surrounded by* $\{\}$*, for example* $\{\mathcal{A}\,2S_3\}$*. In some similar articles where two graphics existed we also used* $\{\{\}\}$ *to denote it, but here we have examples with an infinite number of graphics (the degenerated cases), so we have preferred not to use multiple braces.*

Theorem 4. *Consider the family* **QSE** *of quadratic systems with an invariant ellipse (real or complex). Consider now all the phase portraits that we have obtained for the closure of the corresponding normal forms. The values of the affine invariant* $\mathcal{I} = (I_1, I_2, I_4)$ *given* Diagram 9 *yield a partition of these phase portraits of the family* $\overline{\mathbf{QSE}}$.

Once we have extracted the 45 topologically distinct phase portraits, we provide now a list where we link every representative of the 45 phase portraits with their equivalent ones among the 171 phase portraits obtained from the different parts of the bifurcation diagrams. We also add a symbol from the set $\{\bullet, \circ\}$ to denote if the region belongs to the interior or to the border of **QSE**, respectively. Then, if a phase portrait can only live in the interior or only in the border, we will add also the respective symbol to the phase portrait. If the phase portrait can be obtained both in the interior and also the border, we will add the symbol $\odot$. We always choose as a representative phase portrait, the one coming from the most generic part of the bifurcation diagram with the lowest code (surface and index).

QSE
- $I_1=3$
  - $I_2=4211$ → *Portrait* $\mathcal{A}\,4S_3$
  - $I_2=4311$ → *Portrait* $\mathcal{A}\,V_5$
- $I_1=4$ → *Portrait* $\mathcal{C}\,V_{11}$
- $I_1=8$
  - $I_2=4411$ → *Portrait* $\mathcal{A}\,V_{17}$
  - $I_2=4421$ → *Portrait* $\mathcal{A}\,7S_1$
  - $I_2=4422$ → *Portrait* $\mathcal{A}\,V_{12}$
  - $I_2=4431$ → *Portrait* $\mathcal{A}\,V_{15}$
- $I_1=9$ → *Portrait* $\mathcal{C}\,V_3$
- $I_1=12$ → *Portrait* $\mathcal{A}\,V_3$
- $I_1=16$
  - $I_4=0$ → *Portrait* $\mathcal{A}\,V_1$
  - $I_4=1$ → *Portrait* $\mathcal{A}\,V_4$
- $I_1=18$ → *Portrait* $\mathcal{C}\,V_1$
- $I_1=23$
  - $I_4=0$ → *Portrait* $\mathcal{A}\,V_2$
  - $I_4=1$ → *Portrait* $\mathcal{A}\,V_{18}$
- $I_1=24$ → *Portrait* $\mathcal{C}\,V_5$
- $I_1=30$
  - $I_2=321$ → *Portrait* $\mathcal{A}\,2.4L_2$
  - $I_2=332$ → *Portrait* $\mathcal{A}\,2S_7$
  - $I_2=431$ → *Portrait* $\mathcal{A}\,2S_9$
  - $I_2=521$ → *Portrait* $\mathcal{A}\,2S_2$
- $I_1=34$ → *Portrait* $\mathcal{C}\,2S_1$
- $I_1=37$
  - $I_2=431$ → *Portrait* $\mathcal{A}\,2S_4$
  - $I_2=433$ → *Portrait* $\mathcal{A}\,2S_5$
  - $I_2=541$ → *Portrait* $\mathcal{A}\,2S_3$
- $I_1=44$ → *Portrait* $\mathcal{A}\,2S_1$

DIAGRAM 9. Classification of the phase portraits of systems in **QSE** according to the topological invariants.

- Phase portrait $\mathcal{A}\,V_1^{\odot}$ can be obtained from the regions $\mathcal{A}\,V_1^{\bullet}$, $\mathcal{A}\,V_8^{\bullet}$, $\mathcal{A}\,3S_1^{\circ}$, $\mathcal{A}\,2.2L_1^{\bullet}$, $\mathcal{B}\,V_1^{\bullet}$, $\mathcal{B}\,V_6^{\bullet}$, $\mathcal{B}\,2S_5^{\bullet}$, $\mathcal{B}\,2S_6^{\bullet}$, $\mathcal{C}\,V_{15}^{\bullet}$, $\mathcal{C}\,V_{16}^{\bullet}$ and $\mathcal{C}\,4S_3^{\bullet}$;
- Phase portrait $\mathcal{A}\,V_2^{\odot}$ can be obtained from the regions $\mathcal{A}\,V_2^{\bullet}$ and $\mathcal{A}\,3S_2^{\circ}$;
- Phase portrait $\mathcal{A}\,V_3^{\odot}$ can be obtained from the regions $\mathcal{A}\,V_3^{\bullet}$, $\mathcal{B}\,V_2^{\bullet}$, $\mathcal{B}\,V_3^{\bullet}$, $\mathcal{B}\,V_4^{\bullet}$, $\mathcal{B}\,V_5^{\bullet}$, $\mathcal{B}\,2S_1^{\bullet}$, $\mathcal{B}\,2S_2^{\bullet}$, $\mathcal{B}\,2S_3^{\bullet}$, $\mathcal{B}\,3S_1^{\bullet}$, $\mathcal{B}\,4S_1^{\bullet}$, $\mathcal{C}\,V_{17}^{\bullet}$, $\mathcal{C}\,V_{18}^{\bullet}$, $\mathcal{C}\,V_{19}^{\bullet}$, $\mathcal{C}\,1S_3^{\circ}$, $\mathcal{C}\,1S_6^{\bullet}$, $\mathcal{C}\,3S_4^{\bullet}$ and $\mathcal{C}\,1.2L_5^{\bullet}$;
- Phase portrait $\mathcal{A}\,V_4^{\bullet}$ can be only obtained from the region $\mathcal{A}\,V_4^{\bullet}$;
- Phase portrait $\mathcal{A}\,V_5^{\bullet}$ can be obtained from the regions $\mathcal{A}\,V_5^{\bullet}$, $\mathcal{A}\,V_6^{\bullet}$, $\mathcal{A}\,V_7^{\bullet}$, $\mathcal{A}\,V_9^{\bullet}$, $\mathcal{A}\,V_{10}^{\bullet}$, $\mathcal{A}\,V_{11}^{\bullet}$, $\mathcal{A}\,4S_1^{\bullet}$ and $\mathcal{A}\,4S_2^{\bullet}$;

QSE

- $I_1=47$ → *Portrait* $\mathcal{B}\,2S_8$
- $I_1=50$ → *Portrait* $\mathcal{B}\,2S_4$
- $I_1=60$
  - $I_2=20$ → *Portrait* $\mathcal{C}\,2S_6$
  - $I_2=40$ → *Portrait* $\mathcal{C}\,2S_7$
- $I_1=64$ → *Portrait* $\mathcal{C}\,2S_{10}$
- $I_1=67$ → *Portrait* $\mathcal{B}\,2S_7$
- $I_1=73$ → *Portrait* $\mathcal{A}\,1S_3$
- $I_1=83$ → *Portrait* $\mathcal{A}\,5S_3$
- $I_1=84$
  - $I_4=0$ → *Portrait* $\mathcal{A}\,1S_1$
  - $I_4=1$ → *Portrait* $\mathcal{A}\,1S_2$
- $I_1=97$ → *Portrait* $\mathcal{A}\,5S_1$
- $I_1=98$
  - $I_2=33$ → *Portrait* $\mathcal{A}\,1.2L_2$
  - $I_2=51$ → *Portrait* $\mathcal{A}\,1.2L_1$
- $I_1=122$ → *Portrait* $\mathcal{A}\,2.5L_1$
- $I_1=128$ → *Portrait* $\mathcal{B}\,5S_2$
- $I_1=139$ → *Portrait* $\mathcal{B}\,5S_1$
- $I_1=172$ → *Portrait* $\mathcal{C}\,1.2L_3$
- $I_1=173$ → *Portrait* $\mathcal{B}\,1.2L_1$
- $I_1=174$ → *Portrait* $\mathcal{C}\,P_2$
- $I_1=175$ → *Portrait* $\mathcal{C}\,1.2L_4$
- $I_1=208$ → *Portrait* $\mathcal{B}\,2.5L_3$

Diagram 9 (*contin.*) *Classification of the phase portraits of systems in* $\overline{\mathbf{QSE}}$ *according to the topological invariants.*

- Phase portrait $\mathcal{A}V_{12}^{\bullet}$ can be obtained from the regions $\mathcal{A}V_{12}^{\bullet}$, $\mathcal{A}V_{13}^{\bullet}$, $\mathcal{A}V_{14}^{\bullet}$, $\mathcal{A}4S_4^{\bullet}$, $\mathcal{A}4S_5^{\bullet}$, $\mathcal{B}V_7^{\bullet}$, $\mathcal{B}V_8^{\bullet}$, $\mathcal{B}4S_2^{\bullet}$ and $\mathcal{C}V_8^{\bullet}$;
- Phase portrait $\mathcal{A}V_{15}^{\bullet}$ can be obtained from the regions $\mathcal{A}V_{15}^{\bullet}$, $\mathcal{A}V_{16}^{\bullet}$, $\mathcal{A}V_{19}^{\bullet}$, $\mathcal{A}V_{20}^{\bullet}$, $\mathcal{A}4S_6^{\bullet}$ and $\mathcal{A}4S_7^{\bullet}$.
- Phase portrait $\mathcal{A}V_{17}^{\bullet}$ can be obtained from the regions $\mathcal{A}V_{17}^{\bullet}$, $\mathcal{B}V_9^{\bullet}$, $\mathcal{B}V_{10}^{\bullet}$ and $\mathcal{B}3S_2^{\bullet}$;
- Phase portrait $\mathcal{A}V_{18}^{\bullet}$ can be only obtained from the region $\mathcal{A}V_{18}^{\bullet}$;
- Phase portrait $\mathcal{A}1S_1^{\odot}$ can be obtained from the regions $\mathcal{A}1S_1^{\bullet}$ and $\mathcal{A}1.3L_1^{\circ}$;
- Phase portrait $\mathcal{A}1S_2^{\bullet}$ can be only obtained from the region $\mathcal{A}1S_2^{\bullet}$;

- Phase portrait $\mathcal{A}\,1S_3^{\bullet}$ can be obtained from the regions $\mathcal{A}\,1S_3^{\bullet}$, $\mathcal{A}\,1S_4^{\bullet}$, $\mathcal{A}\,1S_5^{\bullet}$, $\mathcal{A}\,1S_6^{\bullet}$, $\mathcal{A}\,1.4L_1^{\bullet}$ and $\mathcal{A}\,1.4L_2^{\bullet}$;
- Phase portrait $\mathcal{A}\,2S_1^{\bullet}$ can be only obtained from the region $\mathcal{A}\,2S_1^{\bullet}$;
- Phase portrait $\mathcal{A}\,2S_2^{\bullet}$ can be only obtained from the region $\mathcal{A}\,2S_2^{\bullet}$;
- Phase portrait $\mathcal{A}\,2S_3^{\bullet}$ can be only obtained from the region $\mathcal{A}\,2S_3^{\bullet}$;
- Phase portrait $\mathcal{A}\,2S_4^{\bullet}$ can be only obtained from the region $\mathcal{A}\,2S_4^{\bullet}$;
- Phase portrait $\mathcal{A}\,2S_5^{\bullet}$ can be obtained from the regions $\mathcal{A}\,2S_5^{\bullet}$, $\mathcal{A}\,2S_6^{\bullet}$ and $\mathcal{A}\,2.4L_3^{\bullet}$;
- Phase portrait $\mathcal{A}\,2S_7^{\bullet}$ can be obtained from the regions $\mathcal{A}\,2S_7^{\bullet}$, $\mathcal{A}\,2S_8^{\bullet}$, $\mathcal{A}\,2S_{10}^{\bullet}$, $\mathcal{A}\,2S_{12}^{\bullet}$ and $\mathcal{A}\,2.4L_1^{\bullet}$;
- Phase portrait $\mathcal{A}\,2S_9^{\bullet}$ can be obtained from the regions $\mathcal{A}\,2S_9^{\bullet}$ and $\mathcal{A}\,2S_{10}^{\bullet}$;
- Phase portrait $\mathcal{A}\,4S_3^{\bullet}$ can be only obtained from the region $\mathcal{A}\,4S_3^{\bullet}$;
- Phase portrait $\mathcal{A}\,5S_1^{\odot}$ can be obtained from the regions $\mathcal{A}\,5S_1^{\bullet}$, $\mathcal{A}\,5S_2^{\bullet}$, $\mathcal{A}\,1.5L_1^{\bullet}$, $\mathcal{A}\,1.5L_2^{\bullet}$, $\mathcal{A}\,3.5L_1^{\bullet}$ and $\mathcal{A}\,P_1^{\circ}$;
- Phase portrait $\mathcal{A}\,5S_3^{\bullet}$ can be obtained from the regions $\mathcal{A}\,5S_3^{\bullet}$, $\mathcal{A}\,5S_4^{\bullet}$, $\mathcal{A}\,1.5L_3^{\bullet}$ and $\mathcal{A}\,4.5L_1^{\bullet}$;
- Phase portrait $\mathcal{A}\,7S_1^{\bullet}$ can be obtained from the regions $\mathcal{A}\,7S_1^{\bullet}$, $\mathcal{A}\,7S_2^{\bullet}$ and $\mathcal{A}\,4.7L_1^{\bullet}$;
- Phase portrait $\mathcal{A}\,1.2L_1^{\bullet}$ can be only obtained from the region $\mathcal{A}\,1.2L_1^{\bullet}$;
- Phase portrait $\mathcal{A}\,1.2L_2^{\bullet}$ can be obtained from the regions $\mathcal{A}\,1.2L_2^{\bullet}$, $\mathcal{A}\,1.2L_3^{\bullet}$ and $\mathcal{A}\,P_3^{\bullet}$;
- Phase portrait $\mathcal{A}\,2.4L_2^{\bullet}$ can be only obtained from the region $\mathcal{A}\,2.4L_2^{\bullet}$;
- Phase portrait $\mathcal{A}\,2.5L_1^{\bullet}$ can be obtained from the regions $\mathcal{A}\,2.5L_1^{\bullet}$ and $\mathcal{A}\,P_2^{\bullet}$;
- Phase portrait $\mathcal{B}\,2S_4^{\bullet}$ can only be obtained from the region $\mathcal{B}\,2S_4^{\bullet}$;
- Phase portrait $\mathcal{B}\,2S_7^{\odot}$ can be obtained from the regions $\mathcal{B}\,2S_7^{\bullet}$, $\mathcal{C}\,2.2L_1^{\bullet}$, $\mathcal{C}\,2.4L_1^{\circ}$, $\mathcal{C}\,2.4L_2^{\circ}$ and $\mathcal{C}\,P_1^{\circ}$;
- Phase portrait $\mathcal{B}\,2S_8^{\odot}$ can be obtained from the regions $\mathcal{B}\,2S_8^{\bullet}$, $\mathcal{C}\,2S_3^{\bullet}$, $\mathcal{C}\,2S_4^{\bullet}$, $\mathcal{C}\,2S_5^{\bullet}$, $\mathcal{C}\,1.2L_1^{\circ}$, $\mathcal{C}\,1.2L_2^{\bullet}$, $\mathcal{C}\,2.3L_2^{\bullet}$, $\mathcal{C}\,2.4L_3^{\circ}$, $\mathcal{C}\,2.4L_4^{\circ}$, $\mathcal{C}\,2.4L_5^{\circ}$, $\mathcal{C}\,P_3^{\circ}$ and $\mathcal{C}\,P_4^{\circ}$;
- Phase portrait $\mathcal{B}\,5S_1^{\circ}$ can be obtained from the regions $\mathcal{B}\,5S_1^{\circ}$ and $\mathcal{B}\,2.5L_1^{\circ}$;
- Phase portrait $\mathcal{B}\,5S_2^{\circ}$ can be obtained from the regions $\mathcal{B}\,5S_2^{\circ}$ and $\mathcal{B}\,2.5L_2^{\circ}$;
- Phase portrait $\mathcal{B}\,1.2L_1^{\bullet}$ can be obtained from the regions $\mathcal{B}\,1.2L_1^{\bullet}$ and $\mathcal{B}\,1.2L_2^{\bullet}$;
- Phase portrait $\mathcal{B}\,2.5L_3^{\circ}$ can be obtained from the regions $\mathcal{B}\,2.5L_3^{\circ}$ and $\mathcal{B}\,P_1^{\circ}$;
- Phase portrait $\mathcal{C}\,V_1^{\odot}$ can be obtained from the regions $\mathcal{C}\,V_1^{\bullet}$, $\mathcal{C}\,V_2^{\bullet}$, $\mathcal{C}\,V_9^{\bullet}$, $\mathcal{C}\,V_{10}^{\bullet}$, $\mathcal{C}\,1S_1^{\circ}$, $\mathcal{C}\,4S_1^{\bullet}$, $\mathcal{C}\,4S_2^{\bullet}$, $\mathcal{C}\,4S_4^{\circ}$, $\mathcal{C}\,4S_5^{\circ}$ and $\mathcal{C}\,4.4L_1^{\circ}$;
- Phase portrait $\mathcal{C}\,V_3^{\bullet}$ can be obtained from the regions $\mathcal{C}\,V_3^{\bullet}$, $\mathcal{C}\,V_4^{\bullet}$ and $\mathcal{C}\,3S_1^{\bullet}$;
- Phase portrait $\mathcal{C}\,V_5^{\odot}$ can be obtained from the regions $\mathcal{C}\,V_5^{\bullet}$, $\mathcal{C}\,V_6^{\bullet}$, $\mathcal{C}\,V_7^{\bullet}$, $\mathcal{C}\,V_{12}^{\bullet}$, $\mathcal{C}\,V_{13}^{\bullet}$, $\mathcal{C}\,V_{14}^{\bullet}$, $\mathcal{C}\,1S_2^{\circ}$, $\mathcal{C}\,1S_4^{\bullet}$, $\mathcal{C}\,1S_5^{\bullet}$, $\mathcal{C}\,2S_8^{\bullet}$, $\mathcal{C}\,2S_9^{\bullet}$, $\mathcal{C}\,3S_2^{\bullet}$, $\mathcal{C}\,3S_3^{\bullet}$, $\mathcal{C}\,4S_6^{\circ}$, $\mathcal{C}\,4S_7^{\circ}$, $\mathcal{C}\,4S_8^{\circ}$, $\mathcal{C}\,1.4L_1^{\circ}$, $\mathcal{C}\,2.3L_1^{\bullet}$ and $\mathcal{C}\,3.4L_1^{\circ}$;
- Phase portrait $\mathcal{C}\,V_{11}^{\bullet}$ can be obtained from the regions $\mathcal{C}\,V_{11}^{\bullet}$ and $\mathcal{C}\,V_{20}^{\bullet}$;
- Phase portrait $\mathcal{C}\,2S_1^{\bullet}$ can be obtained from the regions $\mathcal{C}\,2S_1^{\bullet}$ and $\mathcal{C}\,2S_2^{\bullet}$;
- Phase portrait $\mathcal{C}\,2S_6^{\bullet}$ can only be obtained from the region $\mathcal{C}\,2S_6^{\bullet}$;
- Phase portrait $\mathcal{C}\,2S_7^{\bullet}$ can only be obtained from the region $\mathcal{C}\,2S_7^{\bullet}$;
- Phase portrait $\mathcal{C}\,2S_{10}^{\bullet}$ can only be obtained from the region $\mathcal{C}\,2S_{10}^{\bullet}$;
- Phase portrait $\mathcal{C}\,1.2L_3^{\circ}$ can be only obtained from the region $\mathcal{C}\,1.2L_3^{\circ}$;
- Phase portrait $\mathcal{C}\,1.2L_4^{\bullet}$ can be only obtained from the region $\mathcal{C}\,1.2L_4^{\bullet}$;
- Phase portrait $\mathcal{C}\,P_2^{\circ}$ can be only obtained from the region $\mathcal{C}\,P_2^{\circ}$.

6. Bifurcation diagram in the space $\mathbb{R}^{12}$ based on the algebraic invariants

Finally we are going to collect all previous results and produce a complete bifurcation diagram in the space $\mathbb{R}^{12}$ based on the algebraic invariants. From this diagram the reader may find which are the relevant invariant polynomials, and apply them to any system and detect if the system possesses or does not possess one of the phase portraits in this classification.

In order to apply the diagram, we must describe the set of invariant polynomials we have used.

First of all we clearly need the conditions for the existence of at least one invariant ellipse. As previously established in [7], the necessary and sufficient conditions for a system in the class **QS** to possess at least one invariant ellipse are expressed in terms of its coefficients. Specifically, [7] defines the following 36 affine invariant polynomials that determine the existence of at least one invariant ellipse:

$$\eta,\ \widetilde{M}, C_2,\ \theta,\ \widetilde{N},\ N_7,\ H_2,\ H_9 - H_{12},\ \mathcal{F},\ \mathcal{T}_3,\ \widehat{\beta}_1 - \widehat{\beta}_8,\ \widehat{\gamma}_1 - \widehat{\gamma}_9,\ \widehat{\mathcal{R}}_1 - \widehat{\mathcal{R}}_6. \tag{12}$$

The explicit forms of the invariant polynomials listed in (12) are provided in [7], where beside the conditions of the existence of an invariant ellipse, there are also the conditions for distinguishing what kind of ellipse we have: real or complex, being or not being a limit cycle.

However for our classification we only need the conditions for the existence of an invariant ellipse and so, we have extracted from [7, Diagrams 1, 2] the conditions to have or not have an invariant ellipse (real or complex). We obtain then a reduced diagram which we present in Diagram 10 below. In this diagram we denote with $\mathcal{E}$ the existence of at least one ellipse (real or complex), and with $\nexists\mathcal{E}$ when it does not exist.

In order to distinguish all the phase portraits we need more algebraic invariants. Some of them are already used for the bifurcation diagrams, concretely $\mathbf{D}$, μ_0, η and $\mathcal{T}_2$ defined in [2] where all the geometrical configurations of singularities were classified and most of the invariant polynomials dealing with singularities are contained. We need two more invariants from the book [2] which have not been needed for the bifurcation diagrams. Concretely we use here $\mathcal{B}$ and $\mathcal{H}$. We have also used the invariant polynomial B_2 which is related with B_1 (for the detection of invariant straight lines) already used in the bifurcation diagram. Both invariants are defined in [9]. Finally we needed to define some new invariants which are listed further below.

$$\begin{aligned}
\widehat{\nu}_1 =& A_7(2A_{15} - A_1A_2),\\
\widehat{\nu}_2 =& 4A_7^2(1624A_8 - 140A_9 + 369A_{10} + 104A_{11} + 599A_{12}) - A_7(27252A_6A_8 + 660A_6A_9\\
& + 8412A_6A_{10} + 10392A_6A_{11} + 10392A_6A_{12} - 244A_3A_{14} + 2211A_4A_{14} + 5718A_5A_{14}\\
& - 1184A_3A_{15} + 495A_4A_{15} + 990A_5A_{15} - 3200A_2A_{16}),\\
\widehat{\nu}_3 =& 4A_8 - 8A_1^2 + 4A_{12},\\
\widehat{\nu}_4 =& 30A_{15}^2 - 17A_8A_{17} - 5A_{10}A_{17} - 5A_{11}A_{17} - 27A_{12}A_{17} - 6A_8A_{18} - 16A_{12}A_{18}\\
& + 16A_8A_{19} + 5A_9A_{19} + 21A_{12}A_{19} - 2A_8A_{20} - 2A_{12}A_{20} - 8A_8A_{21} + 5A_9A_{21}\\
& - 3A_{12}A_{21} + 112A_7A_{25} + 72A_6A_{26} - 264A_7A_{26},\\
\widehat{\nu}_5 =& 16A_1^2A_3 + 48A_6^2 + 48A_6A_7 + 17A_4A_8 - 44A_5A_8 + 4A_4A_{10} + 4A_4A_{11} + 13A_4A_{12} - 36A_5A_{12},\\
\widehat{\nu}_6 =& -2A_3 - 3A_4 + 10A_5,\\
\widehat{\nu}_7 =& A_{19},\\
\widehat{\nu}_8 =& A_{13}.
\end{aligned}$$

The elements A_i for $i = 1, \ldots, 42$ form a minimal polynomial basis of affine invariants of **QS** of degrees up to 12. These elements can also be found in [2].

With all these we can formulate Theorem 3 given in the introduction.

There are two branches of DIAGRAM 11 where the phase portrait has not been completely determined. For one of them the reason is that a non algebraic bifurcation gives place to three different phase portraits, one of them being the phase portrait $\mathcal{A}\,7S_1^{\bullet}$ which has a non algebraic separatrix connection. The second branch is when trying to distinguish $\mathcal{A}\,V_{12}^{\bullet}$ from $\mathcal{A}\,V_{17}^{\bullet}$. We have not been

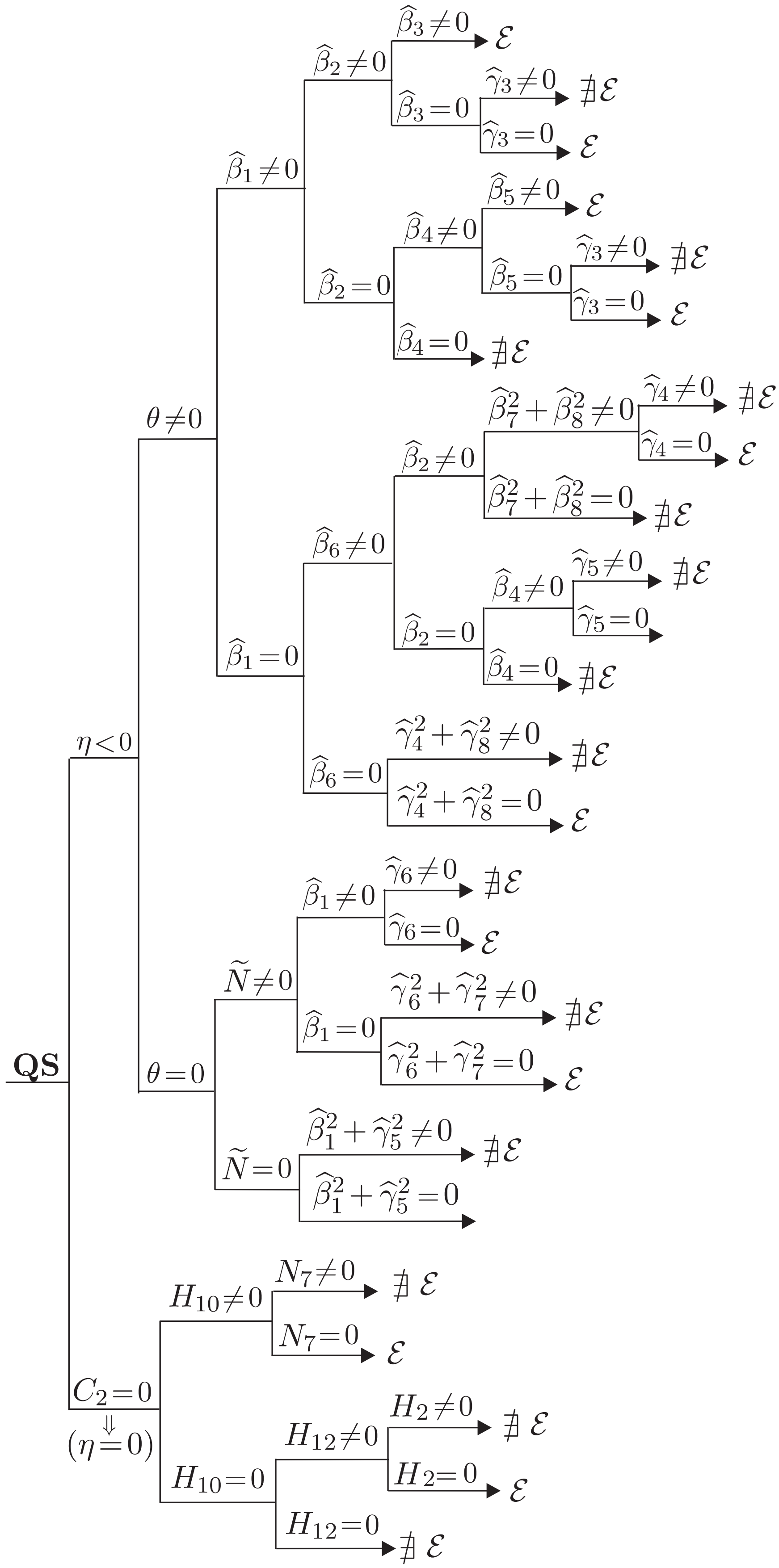

Diagram 10. The conditions for a systems in $\overline{\mathbf{QSE}}$ to possess an invariant ellipse.

able to find an invariant polynomial that splits them, even though we know its specific expression for the particular normal form and slice where it is needed.

Proof. We are going to make the proof of two of the cases to show the algorithm.

We make a list of all the 171 parts of the bifurcation diagram, denoting the name of all the regions, and the corresponding phase portrait. The best way is doing it using an Excel file or anything similar. Then we record the value of the invariants $\mathbf{D}$, μ_0 and $\widehat{\beta}_1$ whether they are negative, positive or zero on each of these parts. At this point we introduce a new invariant $\widehat{\nu}_8$ whose value for the different normal forms is:

$$\begin{aligned} \widehat{\nu}_8^{(\mathcal{A})} =& \widehat{\nu}_8^{(\mathcal{B})} = -m^3(1+m^2+6mn+9n^2)/4, \\ \widehat{\nu}_8^{(\mathcal{C})} =& 0. \end{aligned} \tag{13}$$

That is, if $\widehat{\nu}_8 = 0$ we are either in normal form $(\mathcal{C})$ or in parts where $m = 0$ of normal forms $(\mathcal{A})$ or $(\mathcal{B})$. Alternatively if $\widehat{\nu}_8 \neq 0$ we cannot be in normal form $(\mathcal{C})$. The signs of $\widehat{\nu}_8$ and $\widehat{\beta}_1$ are not relevant, so, if they are not zero, we just record this fact, not the sign. Notice that invariant $\widehat{\beta}_1$ works to distinguish whether we are in normal form $(\mathcal{A})$ or $(\mathcal{B})$.

With these four invariants we reorder the list of regions according to their values from the set neg, not zero, pos, zero. We could continue adding invariants so as to distinguish every two parts of the diagram with the exception of the parts $\mathcal{A}\,7S_1$ and $\mathcal{A}\,7S_2$ from their neighbour parts since these regions are defined by a non algebraic bifurcation. However, we do not need such detail since several regions having the same phase portrait can be ruled by some sets of invariants without the need to separate them further more.

On the top of the reordered list we find now regions $\mathcal{A}\,V_5$, $\mathcal{A}\,V_6$, $\mathcal{A}\,V_7$, $\mathcal{A}\,V_9$, $\mathcal{A}\,V_{10}$, $\mathcal{A}\,V_{11}$, $\mathcal{A}\,4S_1$, $\mathcal{A}\,4S_2$ and $\mathcal{A}\,4S_3$ all of them having $\mathbf{D} < 0$, $\mu_0 < 0$, $\widehat{\nu}_8 \neq 0$ and $\widehat{\beta}_1 \neq 0$. From these regions, all of them have the same phase portrait $\mathcal{A}\,V_5^{\bullet}$ except the last one which has phase portrait $\mathcal{A}\,4S_3^{\bullet}$. So we need to find an invariant (or sets of invariants) which separates region $\mathcal{A}\,4S_3$ from all other, particularly from $\mathcal{A}\,4S_2$. Concretely in this case, we need to make use of $\widehat{\nu}_2$ which is negative for $\mathcal{A}\,V_5$, $\mathcal{A}\,V_6$ and $\mathcal{A}\,4S_1$, and positive in all other regions, followed by $\widehat{\nu}_4$ which is negative for $\mathcal{A}\,V_{10}$, positive for $\mathcal{A}\,V_7$, $\mathcal{A}\,V_9$ and $\mathcal{A}\,V_{11}$, and zero for the remaining two, and finally by $\widehat{\nu}_6$ which is negative for $\mathcal{A}\,4S_3$ and positive for $\mathcal{A}\,4S_2$. Thus we have that phase portrait $\mathcal{A}\,4S_3^{\bullet}$ which only happens in the part $\mathcal{A}\,4S_3$ can be decided by means of invariant polynomials from the phase portrait $\mathcal{A}\,V_5^{\bullet}$ which happens in some other regions. Geometrically, the last invariant $\widehat{\nu}_6$ captures the fact whether the region is below the straight line $m = n$ or above (remember that the bifurcation diagrams and particularly DIAGRAM 1) are drawn topologically correct but not quantitatively).

Let us make another example. Regions $\mathcal{A}\,V_3$, $\mathcal{A}\,V_{16}$, $\mathcal{A}\,V_{15}$, $\mathcal{A}\,4S_6$, $\mathcal{A}\,V_{13}$, $\mathcal{A}\,V_{19}$, $\mathcal{A}\,7S_1$, $\mathcal{A}\,V_{17}$, $\mathcal{A}\,V_{12}$, $\mathcal{A}\,V_{14}$, $\mathcal{A}\,V_{20}$, $\mathcal{A}\,7S_2$, $\mathcal{A}\,4S_4$, $\mathcal{A}\,4S_5$, $\mathcal{A}\,4S_7$ and $\mathcal{A}\,4.7L_1$ share the same invariants $\mathbf{D} < 0$, $\mu_0 > 0$, $\widehat{\nu}_8 \neq 0$ and $\widehat{\beta}_1 \neq 0$. From all of them, only $\mathcal{A}\,V_3$ nas invariant $\widehat{\nu}_1 < 0$ while all others have it positive. Thus phase portrait $\mathcal{A}\,V_3^{\bullet}$ is captured by these invariants and separated from other portraits (even though that same phase portrait may also be obtained from other combinations of invariants like in region $\mathcal{B}\,V_2$ and others). Next we apply invariant $\widehat{\nu}_2$ which is negative for regions $\mathcal{A}\,V_{16}$, $\mathcal{A}\,V_{15}$ and $\mathcal{A}\,4S_6$ and positive for all others. Thus phase portrait is captured by these invariants for the mention regions. Next we apply invariant $\widehat{\nu}_4$ which is negative for regions $\mathcal{A}\,V_{13}$, $\mathcal{A}\,V_{19}$ and $\mathcal{A}\,7S_1$ and positive for all others. We cannot find an invariant to distinguish among the phase portraits obtained from these three regions since they are separated by part $\mathcal{A}\,7S_1$ which belongs to a non-algebraic bifurcation surface. In any case we must continue and we must separate region $\mathcal{A}\,V_{17}$ from $\mathcal{A}\,V_{12}$ which have up to here the same invariants, but different phase portraits. Notice that between both regions we have two branches of the same component of The equation $\mathbf{D} = 0$, thus the sign of $\mathbf{D}$ does not work as a decider, neither the sign of B_1. The decider we have found and that can be

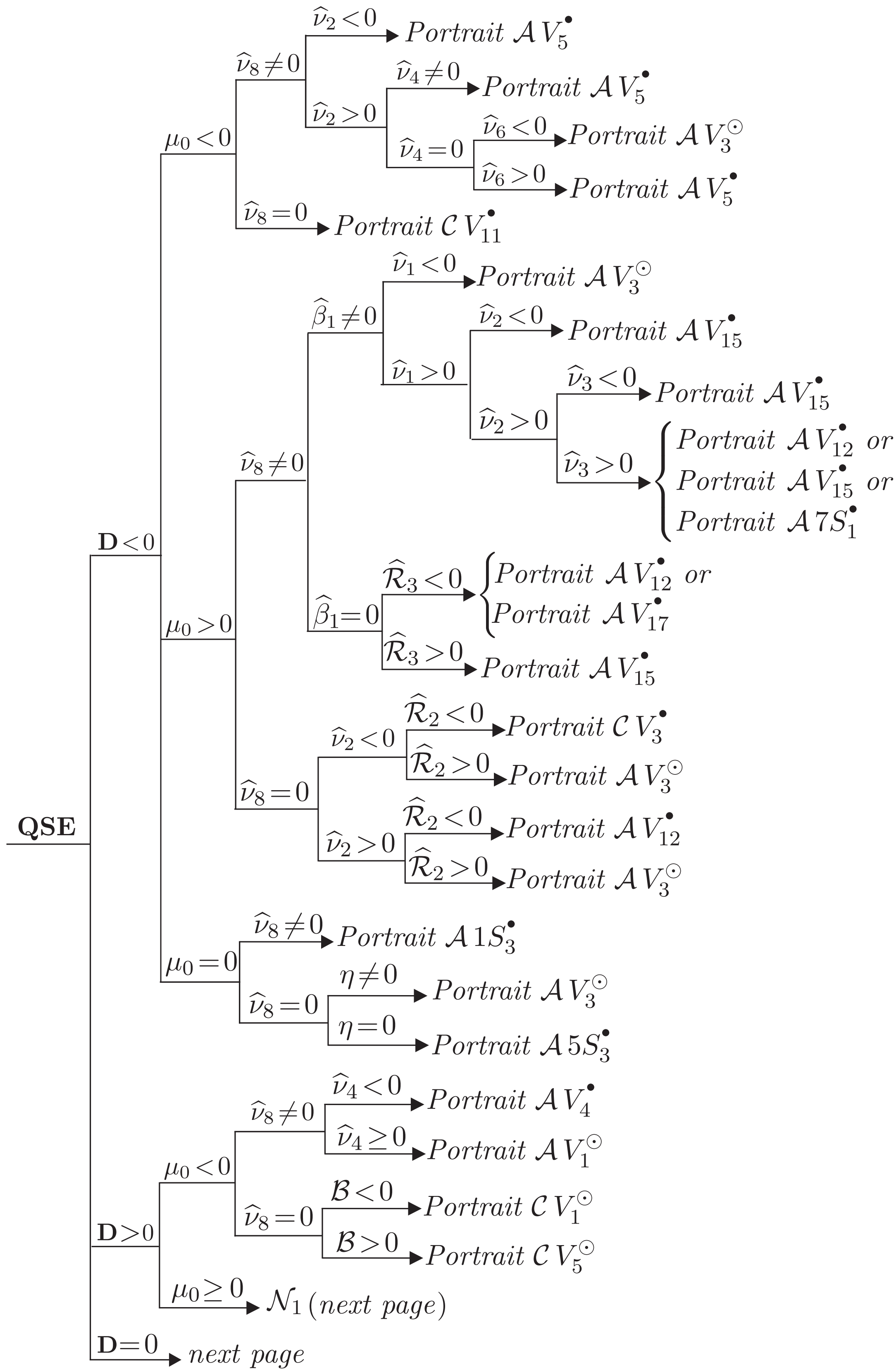

DIAGRAM 11. Bifurcation diagram for the family $\overline{\mathbf{QSE}}$ in the space $\mathbb{R}^{12}$.

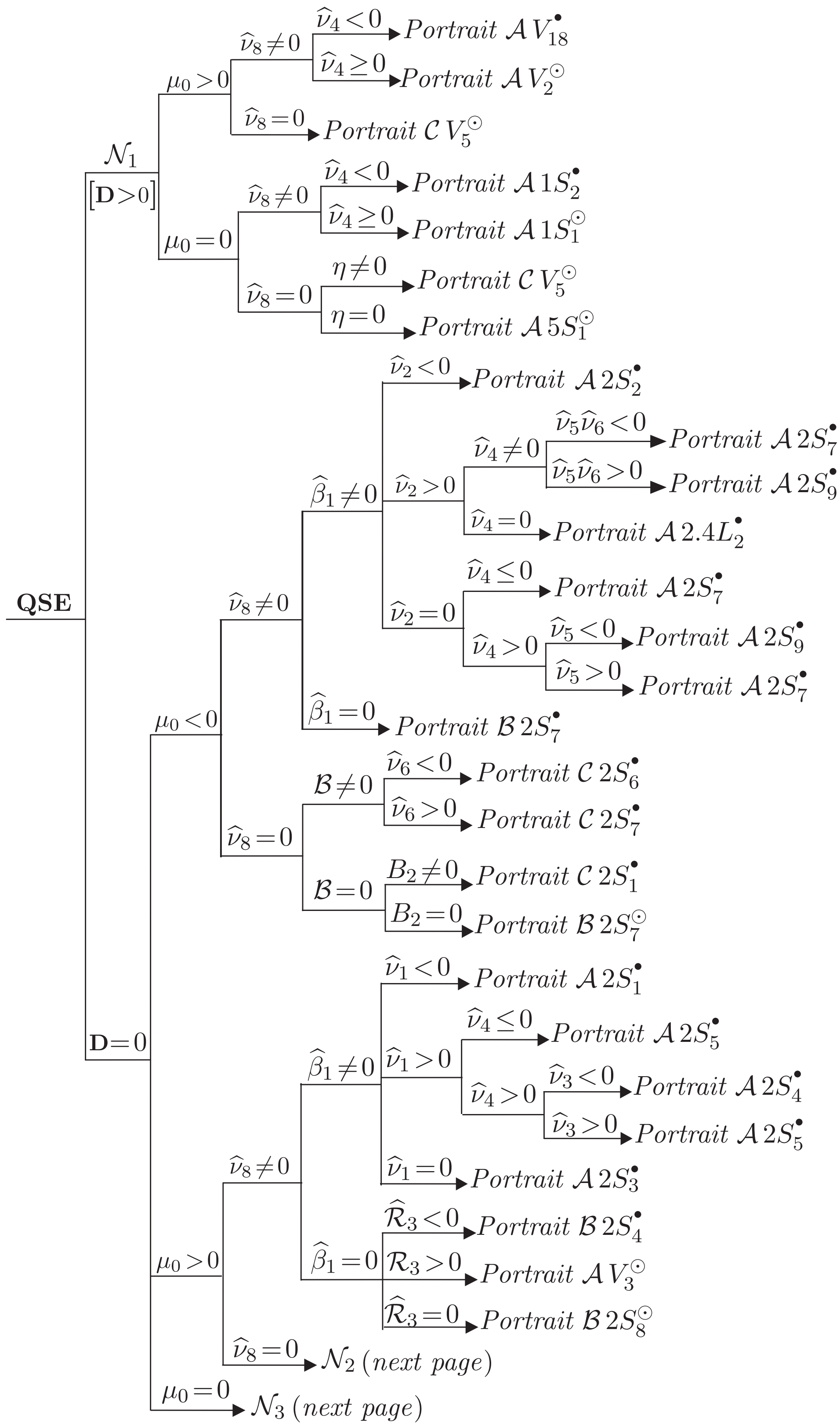

Diagram 11 (*contin.*). Bifurcation diagram for the family $\overline{\mathbf{QSE}}$ in the space $\mathbb{R}^{12}$.

given in an invariant form is the straight line $m=-(1+n^2)/n$ which is always the asymptote of the components of $\mathbf{D}=0$ for any n. And this value is captured by invariant $\widehat{\nu}_3$.

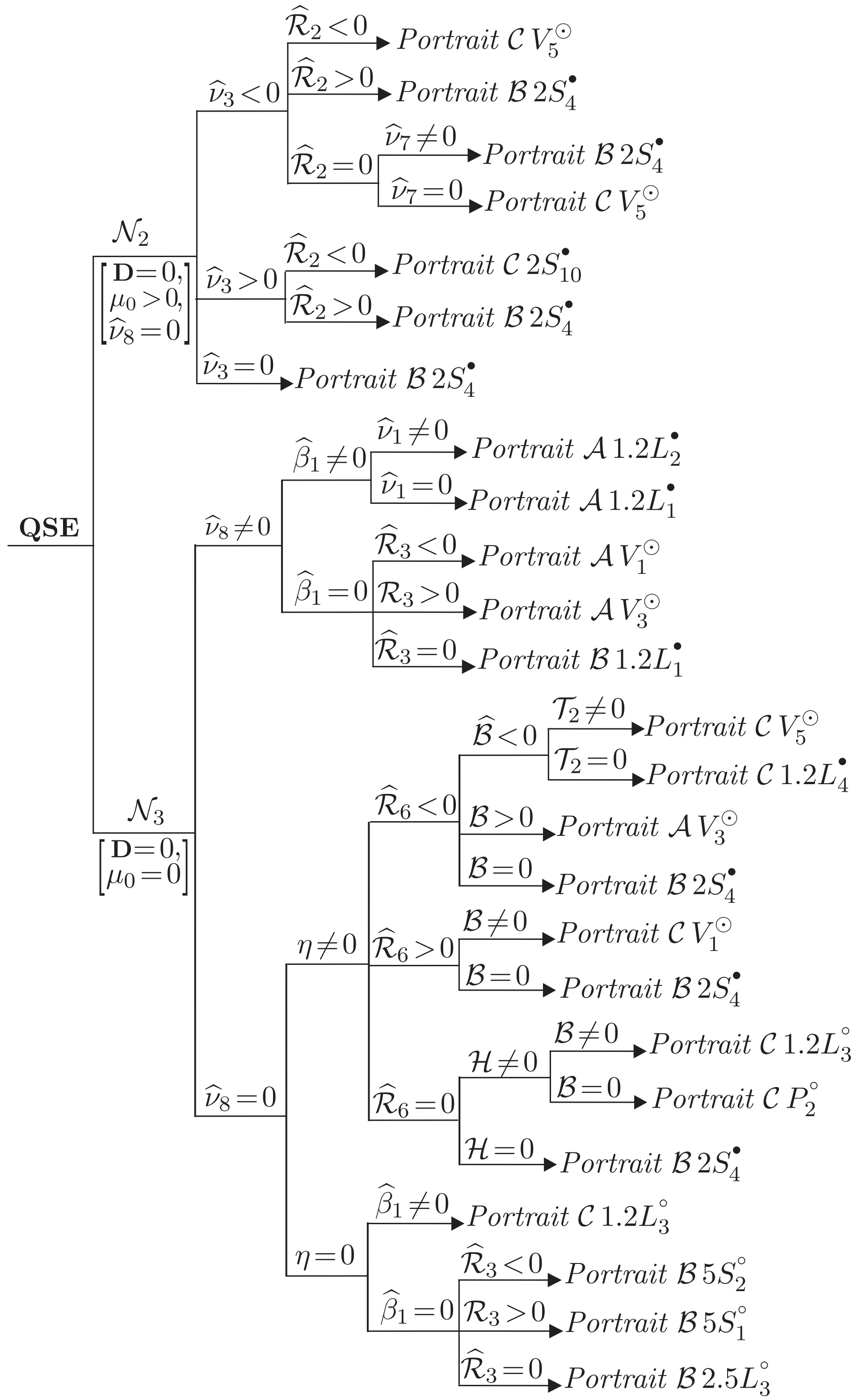

DIAGRAM 11 (*contin.*). Bifurcation diagram for the family $\overline{\mathbf{QSE}}$ in the space $\mathbb{R}^{12}$.

In this way, we have been able to distinguish all the distinct phase portraits, by separating regions with the help of invariants, some of them being the components of some of the already defined invariants, and some others related to some properties of the invariant surfaces like this $\widehat{\nu}_3$.

We have only failed when trying to distinguish regions $\mathcal{B}V_7$, $\mathcal{B}V_8$, $\mathcal{B}V_9$, $\mathcal{B}V_{10}$, $\mathcal{B}3S_2$ and $\mathcal{B}4S_2$, or more precisely, when trying to separate region $\mathcal{B}V_8$ from $\mathcal{B}V_9$ which have different phase portraits. Looking to DIAGRAM 5, it is clear that both regions are separated by the non-trivial component of $\mathbf{D} = 768b^4mn(1 + mn + n^2)^4(1 + m^2 + 2mn + n^2) = 0$, but this trivial component has power even, and thus the sign of $\mathbf{D}$ does not work. We should have found an invariant so as to capture independently the term $1 + mn + n^2$ but we have not succeeded.

There is an Excel file available at "http://mat.uab.cat/∼artes/articles/QSE/QSE.html" which includes all invariants.

So, up to this mentioned case (and the one that cannot be algebraically decided), the bifurcation diagram is done in $\mathbf{R}^{12}$ and the theorem is proved.

□

Acknowledgements.

The first author is supported by the Ministerio de Ciéncia e Innovación (PID2025-168432NB-I00).. The second and the fourth authors are supported by a research project funded within the competition *Stimuarea Excelenţei în Cercetare* 2025-2026 (project code: 25.80012.5007.83SE). The third author is supported by NSERC RN001102.

References

[1] J.C. Artés, J. Llibre, D. Schlomiuk, The geometry of quadratic differential systems with a weak focus of second order, *Internat. J. Bifur. Chaos*, **16**(2006) 3127-3194.

[2] J.C. Artés, J. Llibre, D. Schlomiuk, N. Vulpe, *Geometric configurations of singularities of planar polynomial differential systems* [*A global classification in the quadratic case*]. Birkhäuser/Springer, Cham, [2021], ©2021. xii+699 pp. ISBN: 978-3-030-50569-1; 978-3-030-50570-7

[3] J. C. Artés, J. Llibre, D. Schlomiuk, N. Vulpe, Global topological configurations of singularities for the whole family of quadratic differential systems, Qual. Theory Dyn. Syst., **19** (2020) 51–1-32.

[4] G. Darboux, Mémoire sur les équations différentielles du premier ordre et du premier degré. Bulletin de Sciences Mathématiques, 2eme série, **2**(1) (1878), 60-96; 123-144; 151-200.

[5] F. Dumortier, J. Llibre and J. C. Artés, *Qualitative theory of planar differential systems*, Universitext, Springer-Verlag, New York, 2008, 298 pp.

[6] M.C. Mota, A.C. Rezende, D. Schlomiuk and N. Vulpe, Geometric analysis of quadratic differential systems with invariant ellipses, *Topological Methods in Nonlinear Analysis,* Volume 59, No. 2A, 2022, 623—685, DOI: 10.12775/TMNA.2021.063.

[7] R.D.S. Oliveira, A.C. Rezende, D. Schlomiuk and N. Vulpe, Characterization and bifurcation diagram of the family of quadratic differential systems with an invariant ellipse in terms of invariant polynomials, *Rev. Mat. Complut.* (2021), 53 pp., DOI: 10.1007/s13163-021- 00398-8.

[8] H. Poincaré 1891 Sur l'intégration algébrique des équations différentielles du premier ordre et du premier degré. I. Rend. Circ. Mat. Palermo, **5**, 169–191.

[9] D. Schlomiuk, N. Vulpe, Planar quadratic differential systems with invariant straight lines of total multiplicity four. Nonlinear Anal. 68(4), 681–715 (2008)

[10] Schlomiuk D, Vulpe N., Global topological classification of Lotka-Volterra quadratic differential systems, Electronic Journal of Differential Equations, Vol. 2012 (2012), No. 64, pp. 1–69.

[1] DEPARTAMENT DE MATEMÀTIQUES, UNIVERSITAT AUTÒNOMA DE BARCELONA, 08193 BELLATERRA, BARCELONA, SPAIN

Email address: `joancarles.artes@uab.cat`

[2] STATE UNIVERSITY OF MOLDOVA, VLADIMIR ANDRUNACHIEVICI INSTITUTE OF MATHEMATICS AND COMPUTER SCIENCE, 5 ACADEMIEI STR, CHIŞINĂU, MD-2028, MOLDOVA

Email address: `cristina.bujac@math.md, nvulpe@gmail.com`

[3] Département de Mathématiques et de Statistiques, Université de Montréal

Email address: dana.schlomiuk@umontreal.ca